AFAPL-TR-76-77

ADA033611

WATER INGESTION INTO AXIAL FLOW COMPRESSORS

PURDUE UNIVERSITY
SCHOOL OF AERONAUTICS AND ASTRONAUTICS
WEST LAFAYETTE, INDIANA 47907

AUGUST 1976

TECHNICAL REPORT AFAPL-TR-76-77
FINAL REPORT FOR PERIOD 1 AUGUST 1975 - 31 AUGUST 1976

DDC
DEC 20 1976
A

Approved for public release; distribution unlimited

AIR FORCE AERO PROPULSION LABORATORY
AIR FORCE WRIGHT AERONAUTICAL LABORATORIES
AIR FORCE SYSTEMS COMMAND
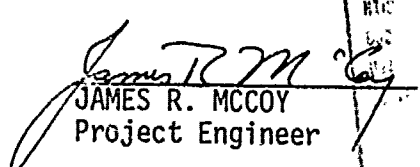WRIGHT-PATTERSON AIR FORCE BASE, OHIO 45433

NOTICE

When Government drawings, specifications, or other data are used for any purpose other than in connection with a definitely related Government procurement operation, the United States Government thereby incurs no responsibility nor any obligation whatsoever; and the fact that the Government may have formulated, furnished, or in any way supplied the said drawings, specifications, or other data, is not to be regarded by implication or otherwise as in any manner licensing the holder or any other person or corporation, or conveying any rights or permission to manufacture, use, or sell any patented invention that may in any way be related thereto.
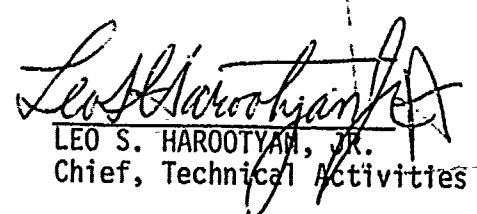
This final report was submitted by Purdue University under contract F33615-74-C-2014. The effort was sponsored by the Air Force Aero Propulsion Laboratory, Air Force Systems Command, Wright-Patterson AFB, Ohio under Project 3145, Task 314532 and Work Unit 31453220 with James R. McCoy/DOY as project engineer in-charge. Dr. S.N.B. Murthy of Purdue University was technically responsible for the work.
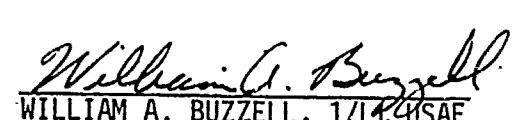
This report has been reviewed by the Information Office, (ASD/OIP) and is releasable to the National Technical Information Service (NTIS). At NTIS, it will be available to the general public including foreign nations.

This technical report has been reviewed and is approved for publication.

JAMES R. MCCOY
Project Engineer

WILLIAM A. BUZZELL, 1/Lt USAF
Task Engineer

FOR THE COMMANDER

LEO S. HAROOTYAN, JR.
Chief, Technical Activities

Copies of this report should not be returned unless return is required by security considerations, contractual obligations, or notice on a specific document.

AIR FORCE - 13 DECEMBER 76 - 100

REPORT DOCUMENTATION PAGE		READ INSTRUCTIONS BEFORE COMPLETING FORM
1. REPORT NUMBER AFAPL-TR-76-77	2 GOVT ACCESSION NO.	3. RECIPIENT'S CATALOG NUMBER
4. TITLE (and Subtitle) Water Ingestion Into Axial Flow Compressors		5. TYPE OF REPORT & PERIOD COVERED Final 1 Aug 75 - 31 Aug 76
		6. PERFORMING ORG. REPORT NUMBER M-WPAFB-T-76-1
7. AUTHOR(s) S.N.B./Murthy, B.A./Reese, C.L./Abernathy and G.T./Arcangeli		8. CONTRACT OR GRANT NUMBER(s) F33615-74-C-2014
9. PERFORMING ORGANIZATION NAME AND ADDRESS Purdue University School of Aeronautics and Astronautics Grissom Hall, West Lafayette IN 47907		10. PROGRAM ELEMENT, PROJECT, TASK AREA & WORK UNIT NUMBERS Program Element 62203F Project/Task 31458220
11. CONTROLLING OFFICE NAME AND ADDRESS Air Force Aero Propulsion Laboratory (DOY) Wright-Patterson AFB OH 45433		12. REPORT DATE August 1976
		13. NUMBER OF PAGES 116
14. MONITORING AGENCY NAME & ADDRESS(If different from Controlling Office)		15. SECURITY CLASS. (of this report) UNCLASSIFIED
		15a. DECLASSIFICATION/DOWNGRADING SCHEDULE

16. DISTRIBUTION STATEMENT (of this Report)

Approved for public release; distribution unlimited

17. DISTRIBUTION STATEMENT (of the abstract entered in Block 20, If different from Report)

18. SUPPLEMENTARY NOTES

19. KEY WORDS (Continue on reverse side if necessary and identify by block number)

Water ingestion, turbomachinery, and jet engines.

20 ABSTRACT (Continue on reverse side if necessary and identify by block number)
The problem of the flow of a gas-liquid mixture through a multi-stage axial compressor originally designed for air flow arises during take-off from a rough runway with water on it and during rain. Preliminary investigations have revealed the problem areas in the fan, L.P., and H.P. compressor stages. The basic aerothermodynamic equations have been deduced in a form suitable for considering development of a computational program.

TABLE OF CONTENTS

ABSTRACT

The problem of the flow of a gas-liquid mixture through a multi-stage axial compressor originally designed for air flow arises during take-off from a rough runway with water on it and during rain. The problem is complicated because of the presence of discrete droplets in a rotating compressor flow field and because of the phase change during compression. In order to alleviate this problem, it is necessary to examine both changes in blade and casing design as well as possible additional controls including variable geometry. The objectives of the investigation presented here are (a) to establish estimates of possible changes in performance of typical aircraft compressors operating with two-phase flow, (b) to determine the governing aerothermodynamic equations for two-phase flow in compressors, and (c) to outline directions in which further research may prove fruitful in this subject. Preliminary investigations have revealed the problem areas in the fan, L.P., and H.P. compressor stages. The basic aerothermodynamic equations have been deduced in a form suitable for considering development of a computational program.

LIST OF FIGURES

(iv)

LIST OF TABLES

NOMENCLATURE

A - droplet (cloud) surface area

A_p - projected frontal area of an equivalent sphere having the same mass as distorted droplet

A_{ps} - projected frontal area of a droplet having statistical mean diameter, d_s

C_D - droplet drag coefficient

C_{wg} - water vapor concentration in gas surrounding droplet (cloud)

C_{ws} - water vapor concentration at surface of droplet (cloud)

c - mixture local sonic velocity

c_1 - constant $\cong 1$

D - drag on a single droplet in a flowing gas

D_b - binary mass diffusivity

$D(\sigma)$ - drag coefficient which depends on size of d_s particle and statistical properties of N_s particles

d - individual droplet diameter

dq_g - heat loss from gas phase (per unit volume of mixture) to surroundings, excluding heat lost directly to liquid phase (joules/Vol$_{\overline{m}}$)

dq_I - heat loss from gas phase (per unit volume of mixture) directly to liquid phase (joules/Vol$_{\overline{m}}$)

(vi)

dq_q — heat loss from liquid phase (per unit volume of mixture) to surroundings, excluding heat lost directly to gas phase (joules/$Vol_{\bar{m}}$)

d_s — statistical mean diameter of a cloud of liquid droplets (Sauter mean diameter)

ds_g — rise in entropy of gas phase (per unit volume of mixture) due to action of body and surface forces on gas phase, excluding those forces imposed by liquid phase (joules/°K $Vol_{\bar{m}}$)

ds_I — rise in entropy of gas phase (per unit volume of the mixture) due to action of forces on gas phase imposed by liquid phase (joules/°K $Vol_{\bar{m}}$)

ds_q — rise in entropy of liquid phase (per unit volume of the mixture) due to action of body and surface forces on liquid phase, excluding those forces imposed by gas phase (joules/°K $Vol_{\bar{m}}$)

$F_{B_{gt}}$ — summation of t-components of all body forces exerted on gas phase per unit volume of mixture (nwt/$Vol_{\bar{m}}$)

$F_{B_{p\ell}}$ — summation of t-components of all body forces exerted on liquid phase per unit volume of mixture (nwt/$Vol_{\bar{m}}$)

F_{I_t} — summation of t-components of all forces exerted on gas phase (per unit volume of mixture) imposed by liquid phase (nwt/$Vol_{\bar{m}}$)

$F_{V_{gt}}$ – summation of t-components of all surface forces exerted on gas phase (per unit volume of mixture), excluding those forces exerted by liquid phase ($nwt/Vol_{\overline{m}}$)

$F_{V_{pt}}$ – summation of t-components of all surface forces exerted on liquid phase (per unit volume of mixture), excluding those forces exerted by gas phase ($nwt/Vol_{\overline{m}}$)

$F(\mu,\rho)$ – defined by equation (2.28)

f – friction coefficient

g – acceleration due to gravity

H_g – total enthalpy of gas phase per unit mass of the gas phase ($joules/Kg_g$)

H.P.   – high pressure

h – standing water depth

h_g – enthalpy of gas phase per unit mass of gas phase ($joules/Kg_g$)

h_h – average interfacial heat transfer coefficient of droplet (cloud)

h_m – average interfacial mass transfer coefficient of droplet (cloud)

I – rothalpy ($I_g = h_g + \dfrac{W_g^2}{2} - \dfrac{U_g^2}{2}$)

k – thermal conductivity of fluid surrounding droplet (cloud)

k_e — the effective thermal conductivity of mixture

L — direction tangent to computing station at a particular streamline (Figure 4.1)

L.P. — low pressure

L.P.C. — low pressure compressor

m — mass

$\dot{m}$ — mass flow rate

$m(n)$ — the nth moment of droplet distribution function

m, θ, n — intrinsic coordinate system defined in Figure 4.1

$\dot{m}_v$ — water vapor mass production rate per unit volume of mixture (gm/sec $Vol_{\bar{m}}$)

m.w. — molecular weight

m_w — the amount of water sprayed (per unit distance of wheel travel) behind the wheel

$\dot{m}_w$ — time rate of the "pumping" of water by tire

N_s — statistical droplet number density of a cloud of liquid droplets with statistical mean diameter, d_s

Nu — Nusselt number

$n(\sigma_r)$ — droplet distribution function

nwt — Newtons

P — pressure

$\bar{P}$ — shaft work (per unit time per unit volume of mixture) done on phase designated, $\bar{P}_g$ or $\bar{P}_p$

Pe_h — heat transfer Péclét number

Pe_m — mass transfer Péclét number

P_0 — total pressure

P_{0_2}/P_{0_1} — compressor total pressure ratio

Pr — Prandtl number

$p(d)$ — probability of droplet having diameter between d and $(d + \delta d)$

q'_{gt} — heat transferred from gas phase (t-direction), excluding heat transferred directly to liquid phase (watts/meters$^2_{\bar{m}}$)

q'_{lt} — heat transferred from gas phase (t-direction) to liquid phase directly (watts/meters$^2_{\bar{m}}$)

q'_{pt} — heat transferred from liquid phase (t-direction) to surroundings, excluding heat transferred directly to gas phase (watts/meters$^2_{\bar{m}}$)

Re_p — particle Reynolds number

R_g — gas phase gas constant

RPM(rpm) — revolutions per minute of compressor rotor

r — compressor radial coordinate defined in Figures 4.1 and 4.2

(x)

r_c — stream surface meridional radius of curvature

r, θ, z — cylindrical coordinate system defined in Figure 4.2

Sc — Schmidt number

Sh — Sherwood number

T — temperature

T_{gp} — mass averaged gas phase-liquid phase temperature (°K)

T_0 — total temperature

T_{0_2}/T_{0_1} — compressor total temperature ratio

U — magnitude of local blade rotational velocity vector

$\bar{U}$ — local blade rotational velocity vector

U_c — speed of undercarriage of an aircraft wing

$U_0 \hat{e}_x$ — mean fluid velocity prior to addition of d_s size test particle

U_p — total internal energy of liquid phase (joules/Kg_p)

u_E — relative superficial velocity $(1 - \sigma_v)$

u_p — internal energy of liquid phase per unit mass of liquid phase (joules/Kg_p)

V — magnitude of the absolute velocity vector

$\bar{V}$ — absolute velocity vector

W — magnitude of the relative velocity vector

$\bar{W}$ — relative velocity vector

We	- Weber number
W_s	- saturation mass fraction of water vapor at given values of temperature and pressure
X	- defined by equation (2.26)
Y	- defined by equation (2.25)
y_B	- defined in Figure A.I.1
$\dot{y}_B$	- time derivative of y_B
Z	- defined by equation (2.27)
α	- thermal diffusivity
$\bar{\alpha}$	- defined by equation (2.12)
α_1	- rotor absolute flow inlet angle
α_2	- rotor absolute flow exit angle
β	- defined by equation (2.22)
β_1	- rotor relative flow inlet angle
β_2	- rotor relative flow exit angle
γ	- specific heat ratio
γ_c	- defined in Figure 4.1
ϵ	- blade row mean flow deflection
η	- compressor efficiency
η_1	- defined by equation (A.I.3)

n_2 - defined by equation (A.I.4)

μ - absolute viscosity

ξ - interfacial viscosity

ρ - density

σ - droplet surface tension

σ_m - mass of particulate liquid (liquid phase) per unit mass of mixture

σ_r - individual droplet radius

σ_v - volume of particulate liquid (liquid phase) per unit volume of mixture

Φ_g - heat generated (per unit time per unit volume of mixture) in gas phase due to viscous dissipation caused by all sources except liquid phase (watts/$Vol_{\bar{m}}$)

Φ_I - heat generated (per unit time per unit volume of mixture) in gas phase due to viscous dissipation caused by liquid phase (watts/$Vol_{\bar{m}}$)

Φ_p - heat generated (per unit time per unit volume of mixture) in liquid phase due to viscous dissipation caused by all sources except gas phase (watts/$Vol_{\bar{m}}$)

ϕ - defined in Figure 4.1

ϕ_1 - angle between radius vector and m-direction

ϕ_2 - angle between radius vector and n-direction

(xiii)

ω - angular velocity of compressor rotor

$\bar{\omega}$ - blade row mean total pressure loss

$(\ )_a$ - pertaining to air

$(\ )_g$ - pertaining to gas phase (gas phase = air + water vapor)

$(\ )_{\bar{m}}$ - pertaining to mixture (gas phase + liquid phase)

$(\ )_{m,\theta,n;\ r,\theta,z}$ - pertaining to m,θ,n; r,θ, or z direction respectively,
(e.g., V_{gm} is magnitude of gas phase velocity in m-
direction and V_{pz} is magnitude of liquid phase velocity
in z-direction)

$(\ )_p$ - pertaining to particulate liquid phase (particulate
liquid phase = liquid phase)

$(\ )_w$ - pertaining to water

1. INTRODUCTION

Two-phase flow in turbomachinery is of interest in a number of technological problems, e.g. rain ingestion into compressors on ground or during flight, condensation in steam turbines, pumping of crude oil, circulation of coolants in nuclear reactors, etc. The principal interest in this Report is in the problem of air-water mixture flow through diffusers and compressors. In gas turbines installed in aircraft, the problem of water ingestion into the engine is known to lead to serious consequences, both by reducing the stall margin and occasionally leading to after-burner blowout (Ref. 1). The ingestion of water may arise during take-off from puddles on rough runways or during flight through a rainfall. It is unclear at the moment if the problems of surge and blow-out can be removed with simple bleed-type controls or if one has to employ, for instance, casing treatment or even redesign of selected blading in extreme cases. It is possible that no general solution can be obtained for all types of compressors and all types of water ingestion, but one may be able to establish general guidelines for design, control, and operation of compressors. Such general guidelines may then be adapted to suit given compressor configurations.

No adequate theory exists for the motion of a two-phase fluid through a compressor. The compressor of interest in this Report is a rotating machine, for e.g., an axial flow compressor. The increase in pressure arises on account of work done on the fluid. In the absence of rotation and work input to the fluid, one can consider a simple diffuser with an adverse pressure gradient. There is no adequate theory for two phase flow even through such a diffuser

1

The two-phase flow of interest in this Report has two basic
complexities:

    (a) In the air-water mixture flow, water is in the form of discrete
        droplets which may undergo break-up or coalescence during
        motion.

    (b) When work is done on the fluid, water may undergo a phase change,
        leading ultimately to the fluid becoming an air-steam mixture.

The aerothermodynamics of two-phase flow thus becomes quite complicated.

    Considering an axial compressor, such as for e.g. the TF-30, several
additional complexities arise in the flow:

    (a) Alternating rotating and stationary blade rows.

    (b) Division of the compressor into the L.P. and H.P. sections.

    (c) Flow entry geometry at the inlet to the compressor.

Taken together with the complexities of two-phase flow, the foregoing
presents a formidable problem.

    At this time, there are no experimental studies of a sufficiently
detailed nature to provide some guidance for theory and analysis. The
experimental studies again present several complicated problems on
account of the rotation in the fluid (both centrifugal and Coriolis
forces have to be included appropriately) and the presence of the dis-
crete phase. For example, the combined effects of centrifuging and
coalescence can lead to a film flow of water along the casing of a
compressor and it is important to establish the possibility of such a
film flow both from an analytical and a practical point of view.

An interesting aspect of the presence of water at entry to the compressor is the _____ in humidity of air throughout the compressor. A measure of _____ is what may be termed the "Saturation Mass Fraction of Water", _____ as the mass of water in a pound mass of air at saturation under given conditions of pressure and temperature. Thus, if W_s is the satur__ __ mass fraction of water at given values of ambient temperature and pressure, one can write (Ref. 2)

$$W_s = 0.6219 \, P_s/(P - P_s) \qquad (1.1)$$

where

$$0.6219 = \frac{\text{Molecular Weight of Water Vapor}}{\text{Molecular Weight of Dry Air}}$$

P = air-water vapor mixture pressure

P_s = partial vapor pressure of water at conditions of saturation.

W_s, by definition, is a local parameter. If one considers standard atmospheric conditions at entry to the P&W TF-30 compressor and the local conditions at the exit of stages 1, 2, 3, 4, 5, and 6, one can tabulate the values of W_s at the local conditions as shown in Table 1.1. Thus, at a pressure of 39.71 psia and temperature of 419.78°K, the value of W_s is 0.9821, which means that the amount of water that can be held in 1 lb of air under saturated conditions is 0.9821 lb.

One should however not be misled by the possible values of W_s. In actual practice, the attainment of equilibrium conditions with respect to humidity requires a finite length of time which in turn depends upon the size, number and geographical distributions of droplets, and their convection velocity. There is no clear method of establishing the increase in

3

Table 1.1

Local Values Of W_s Under Saturated Conditions*

Stage	Temperature	Pressure	W_s
	°K	psia	
Inlet	271.41	11.90	0.0040
1	302.68	16.97	0.0217
2	332.21	22.59	0.0754
3	356.64	27.44	0.1778
L.P.C. Inlet	365.54	24.74	0.2778
4	379.39	32.04	0.3529
5	419.78	39.71	0.9821
6	434.98	46.77	>1 Not Defined

*Fan Data Taken At Diameter Equal to Outer Diameter Of L.P.C. Capture
Area. L.P.C. Data Taken At Blade Tips.

humidity of the air in the presence of water droplets over a unit period of time even in a simple duct flow. In a complicated flow such as that in a compressor, the problem becomes practically insurmountable. However, one has to allow for some change in the liquid water content along the compressor on account of changes in the humidity of air.

The objective of this Report is three-fold: (1) To conduct a performance estimation study on a selected compressor for the general effects of two-phase flow in the compressor when it has been originally designed for air flow only; (2) To establish the basic governing equations for the aerothermodynamics of two-phase flow through a compressor; and (3) To outline a program of theoretical and experimental studies that can lead to an engineering solution to the problem of water ingestion into installed engine compressors.

1.1 Outline of Report

In order to set the background for the problem of two-phase flow through a compressor we present in Section 2 some basic two-phase flow considerations. The presence of water in discrete phase introduces in a compressor problems of heat and mass transfer and of phase change. We therefore discuss thermo-physical and transport considerations.

In Section 3 some preliminary results are presented on the changes in the overall performance of selected compressors when two-phase flow is introduced into them. A general discussion on aerothermodynamics of two-phase flow through a compressor is presented in Section 4.

Finally, an outline for future studies is developed in Section 5 with a special emphasis on experimental studies.

5

2. TWO-PHASE FLOW CONSIDERATIONS

The subject of two-phase flow is of interest in many technologies and several reviews of the subject are available (Refs. 3-7) although the subject is extremely complicated and presents many unsolved problems. We shall concentrate here on those aspects of two-phase flow that are specialized to the current investigation.

The two-phase flow of interest in this investigation is air carrying water droplets. The water droplets are the result of rain ingestion or of water sprayed into the inlet during take-off from puddles on uneven runways.

The presence of water alters the humidity of air at entry and in fact throughout the compressor with changes in temperature and pressure so long as water is present in the flow

The first consideration when water is present in discrete droplet form is the size and number density distribution. If the water is ingested on account of rain, the initial size and number density distribution can be related in a very approximate fashion to the rain droplet size distribution (Refs. 8-9). When water is splashed into the compressor inlet from runway puddles, one can make a preliminary estimate of the amount of water that may be splashed by the wheel on account of the relative motion between the water surface and the adjoining air flow (see Appendix I). There is considerably greater ambiguity in the spray characteristics (Ref. 10). In addition to the uncertainties in the spray envelope from the wheel, there is also the difficulty of determining the influence of inlet geometry and flow on the actual ingestion process.

6

The inlet flow itself is altered in many cases by the proximity of the ground. Until such time when better data become available on droplet size and number characteristics, the only feasible approach is to assume that distributions of statistical mean diameter and number density may be treated as parameters at the inlet to the compressor.

Upon entry into the compressor, the size and number density distributions of droplets alter continuously on account of the following.

(i) break-up and coagulation; and

(ii) evaporation.

The break-up and coagulation arise on account of the motion in a moving and generally rotating environment in the presence of gravitational action. The evaporation requires the droplets to become heated to the boiling point at the local pressure and then to evaporate with the absorption of latent heat. The evaporation is a strongly rate dependent process and several characteristic length and time scales are involved. At this stage the only feasible approach to take in such problems is to include the break-up and evaporation processes in the changes in the statistical mean diameter and number density locally along the streamlines.

The second consideration when water is present in discrete droplet form is the distribution of velocities for the different droplets. We assign a single mean velocity for each group of droplets with an assigned mean statistical diameter. We are thus avoiding consideration of the motion of individual droplets in any group.

The third consideration arises from the fact that water droplets introduce the drag of droplets into the momentum balance of the air flow. The drag is based here, by assumption, on the Reynolds number calculated

7

with respect to the statistical mean diameter and the relative velocity of the droplets with respect to air flow velocity. The drag of N_s droplets is taken as N_s times the drag of one d_s size particle.

The fourth and last consideration to be taken into account here is the difference between the compressibility of the mixture and the compressibility of air. The acoustic velocity in the mixture is different from that in the air and the local Mach number of the mixture at any location is therefore based on the acoustic velocity in the mixture.

In view of the foregoing considerations, some tentative bases have been selected to take into account the various processes. They are elucidated in the following.

2.1 Water-Phase Continuum

The water content in the mixture is treated as a continuum in the general equations of motion along with air and the mixture. The water content in a unit volume at any location is assigned a value σ_v by volume. Continuity is thus assumed for $(1 - \sigma_v)$ of air and σ_v of water. It should be pointed out that σ_v changes along the flow and hence is a dependent variable in the flow equations.

In spite of the assumption of continuum for the water droplets, it is assumed that the water droplets do not contribute to the local pressure based on the reasoning that the droplets are not distributed randomly enough.

It may be pointed out here that for certain purposes, the droplets are considered as discrete entities. Three processes for which it is considered necessary to discretize the droplets are (1) the exchange of

8

momentum between the air and the droplets, (2) the evaporation of the droplets, and (3) the break-up and agglomeration of droplets.

2.2 Compressibility of the Mixture

The acoustic velocity in a droplet-laden air flow is given by the following relation (Ref. 11).

$$c = \left[\left\{ (1 - \sigma_v)\rho_g + \sigma_v \rho_p \right\} \left\{ \frac{1 - \sigma_v}{\rho_g c_g^2} + \frac{\sigma_v}{\rho_p c_p^2} \right\} \right]^{-\frac{1}{2}} \tag{2.1}$$

where

c = mixture sonic velocity

σ_v = particulate liquid volume fraction = volume of particulate liquid per unit volume of mixture

ρ = density

$(\ )_g$ = pertaining to gas phase

$(\ )_p$ = pertaining to particulate liquid phase.

Equation (2.1) is presented graphically in Figure 2.1 for standard atmospheric conditions and for a range of σ_v from 0.00 to 0.10; the range over which this report is interested.

2.3 Distribution of Droplet Size and Number Density

The volume σ_v of water in a unit volume of the mixture at any location is specified by the following relation.

$$\sigma_v = \frac{\pi}{6} d_s^3 N_s \tag{2.2}$$

where

d_s = statistical mean droplet diameter of a cloud of liquid droplets

N_s = statistical droplet number density of a cloud of liquid droplets with a statistical mean diameter, d_s.

9

For our purposes the statistical mean droplet diameter is taken as the Sauter mean diameter (Ref. 12)

$$d_s = \int_0^{d_{max}} d^3 p(d) dd / \int_0^{d_{max}} d^2 p(d) dd \qquad (2.3)$$

where

    d = an individual droplet diameter

    $p(d)$ = the probability of a droplet having a diameter between d
          and $(d + \delta d)$.

It should be noted that a droplet with diameter equal to the Sauter mean diameter has the same surface area to volume ratio as the entire spray.

It should be recognized that in addition to σ_v, d_s and N_s also may change along the flow depending upon droplet break-up and evaporation processes. Thus, when σ_v changes, there may also arise a change in d_s and then one can assign a value for N_s corresponding to the changed values of σ_v and d_s.

At entry to the compressor, a radial and circumferential distribution of σ_v and d_s is specified, although under an axisymmetric assumption the circumferential variation in distribution can be neglected.

2.4 Break-up of Droplets

A droplet is assumed to breakup when the Weber number becomes of the order of ten. The Weber number based on d_s is defined by the relation (Ref. 13):

$$We = \rho_g (V_g - V_p)^2 d_s / \sigma \qquad (2.4)$$

10

where

> We = Weber number
>
> V = velocity
>
> σ = droplet surface tension.

It may be noted again that σ_v is not affected by the break-up locally, although the change in σ_v from position to position is affected by the droplet break-up.

2.5 Formation of a Film of Water

The combined effect of droplet agglomeration, centrifugal action and gravitational action can lead to the formation of a stream of water at the casing wall. There is no experimental evidence for this and it is a very important question both from the point of view of fluid dynamics and the possible arrangements required for the removal of water. It is extremely difficult to establish the formation of a film of water on an analytical basis.

We assume that when the value of σ_v reaches a large enough value for the mixture to be treated as a bubbly mixture, there arises a film. Such a value of σ_v is estimated to be 0.40 for tap water and air and 0.90 for "pure" water and air (Ref. 14) at a pressure of one atmosphere.

2.6 Drag on a Cloud of Droplets

The drag on a spherical droplet carried in an airflow is a function of its Reynolds number based on the droplet diameter (d_s) and the droplet velocity relative to that of air velocity in the vicinity of the droplet. If we assume $d_s = 1.0$ mm and a relative velocity of 10 m/sec., the Reynolds number becomes 688 at standard atmospheric temperature and

11

pressure. The drag on a single droplet may then be written as follows (Ref. 15).

$$D = 0.5 \, C_D \, \rho_g (V_g - V_p)^2 A_p \qquad (2.5)$$

where

$$
\begin{aligned}
C_D &= 24.0 \, Re_p^{-1.0} & Re_p &< 0.5 \\
C_D &= 27.0 \, Re_p^{-0.84} & 0.5 &< Re_p < 70.0 \\
C_D &= 0.414 \, Re_p^{0.1433} & 70.0 &< Re_p < 1.3 \times 10^6 \\
C_D &= 3.0 & 1.3 \times 10^6 &< Re_p.
\end{aligned}
\qquad (2.6)
$$

The particulate Reynolds number is defined as follows.

$$Re_p = \rho_g \, d_s \left| V_g - V_p \right| / \mu_g \qquad (2.7)$$

where

C_D = particle drag coefficient

A_p = projected frontal area of an equivalent sphere having the same mass as the droplet.

The drag on a cloud of droplets becomes much more complicated to estimate because of (a) the mutual interaction between the droplets and (b) the arbitrariness of the direction of motion of different droplets at different times in the vicinity of any one droplet. References 16-28 provide a short bibliography on this subject. Two examples of drag correlations are given here, one due to Refs. 16 and 21, and the other due to Ref. 22.

2.6.1 Soo's Drag Coefficient Using Ergun's Pressure Drop Equation

Drag of a cloud of N_s droplets = N_s x the drag of one d_s size particle

$$= N_s \times 0.5 \, C_D \, \rho_g (V_g - V_p)^2 A_{ps} \qquad (2.8)$$

12

where

A_{ps} = projected frontal area of a droplet having the statistical mean diameter d_s.

$$C_D = \frac{200 \, \sigma_v \, \mu_g}{(1 - \sigma_v) d_s \, u_E \, \rho_g} + \frac{7}{3(1 - \sigma_v)} \tag{2.9}$$

where

$$0.08 \le \sigma_v \le 0.60 \quad \text{and} \quad 1.0 \le \frac{Re_p}{\sigma_v} \le 3000.0$$

μ = absolute viscosity

u_E = relative superficial velocity/$(1 - \sigma_v)$.

The relative superficial velocity is the relative gas flow, $(V_g - V_p)$, based upon the unobstructed flow area, i.e., the flow area when no droplets are present.

2.6.2 Tam's Formula for the Drag Exerted on a Particle in a Cloud of Spherical Particles

Drag on one d_s size particle = $D(\sigma) \, U_0 \, \hat{e}_x$ \hfill (2.10)

where

$U_0 \, \hat{e}_x$ = the mean fluid velocity before the addition of the d_s size particle

$D(\sigma)$ = a drag coefficient which depends on the size of the d_s particle and the statistical properties of the N_s particles

$$D(\sigma) = 3\pi \, \mu_g \, d_s [1 + \frac{\bar{\alpha} \, d_s}{2} + \frac{1}{12}(\bar{\alpha}^2 \, d_s^2)] \tag{2.11}$$

$$\bar{\alpha} = \frac{6\pi \, m_2 + [36\pi^2 \, m_2^2 + 24\pi \, m_1(1 - \frac{3\sigma_v}{2})]^{\frac{1}{2}}}{2 - 3\sigma_v} \tag{2.12}$$

$$m(n) = \int n(\sigma_r)\sigma_r^n \, d\sigma, \tag{2.13}$$

13

and where

σ_r = particle radius

$n(\sigma_r)$ = particle distribution function

$m(n)$ = the nth moment of the particle distribution function

$$0.0 \leq \sigma_v \leq 0.50 \qquad 0.0 < Re_p \leq 2.0.$$

2.7 Heat (Mass) Transfer Between a Cloud of Droplets and the Surrounding Fluid

In our case of interest, the interfacial transfer of heat and mass between a single droplet and the surrounding fluid is primarily due to forced convection. Free convection and radiative (heat) transfer are neglected. The transfer rates may be determined by the following.

$$\text{Heat Transfer Rate} = h_h A(T_p - T_g)$$

$$\text{Mass Transfer Rate} = h_m A(C_{ws} - C_{wg})$$

(2.14)

where

h_h = average heat transfer coefficient for the droplet (cloud)

h_m = average mass transfer coefficient for the droplet (cloud)

A = droplet (cloud) surface area

T = temperature

C_{ws} = water vapor concentration at surface droplet (cloud)

C_{wg} = water vapor concentration in fluid flowing around droplet (cloud).

When the relative velocity between a single droplet and the surrounding fluid approaches zero the following relationship is used to determine the transfer rates (Ref. 29).

$$\left.\begin{array}{l} Nu = 2.0 \\ Sh = 2.0 \end{array}\right\}$$

(2.15)

14

where

Nu = Nusselt number = $h_n d_s/k$

Sh = Sherwood number = $h_m d_s/D_b$

k = thermal conductivity of the fluid surrounding the droplet (cloud)

D_b = binary mass diffusivity.

The convective interfacial heat and mass transfers are a function of the respective Péclét number, and the internal circulation of the droplet. The Péclét numbers are defined as follows:

$$Pe_h = Re_p \times Pr = \left| V_g - V_p \right| d_s/\alpha_g \tag{2.16}$$

$$Pe_m = Re_p \times Sc = \left| V_g - V_p \right| d_s/D_b \tag{2.17}$$

where

Pe_h = heat transfer Péclét number

Pe_m = mass transfer Péclét number

Pr = Prandtl number = $\mu_g/\rho_g \alpha$

Sc = Schmidt number = $\mu_g/\rho_g D_b$

α = thermal diffusivity of the fluid surrounding the droplet (cloud).

Again assuming d_s = 1 mm and a relative velocity of 10 m/sec, Pe_h = 498, and Pe_m = 391 at standard atmospheric conditions.

When the particulate phase changes from discrete droplets to bubbles the internal circulation varies from zero to a maximum. Fluid droplets are considered to have an intermediate amount of internal circulation. The presence of surfactant (surface reactant) impurities contaminates

15

the gas-fluid particle interface and also tends to reduce the internal circulation in droplets and bubbles. This in turn considerably reduces the rates of interfacial transfer.

References 30 and 31 provide a summary of a large number of analytic and correlated results for single particle interfacial transfer. Three such results follow.

Friedlander (Ref. 32).

$$\left. \begin{array}{l} Nu = 2[1 + \dfrac{Pe_h}{4} + \dfrac{Pe_h^2}{12} + \ldots] \\[3mm] Sh = 2[1 + \dfrac{Pe_m}{4} + \dfrac{Pe_m^2}{12} + \ldots] \end{array} \right\} \qquad (2.18)$$

These results apply for no internal circulation, small Péclét numbers, and small particle Reynolds numbers.

Levich (Ref. 33).

$$\left. \begin{array}{l} Nu = 0.998\, Pe_h^{1/3} + 2 \\[3mm] Sh = 0.998\, Pe_m^{1/3} + 2 \end{array} \right\} \qquad (2.19)$$

Levich's results apply for no internal circulation, large Péclét numbers, and small particle Reynolds numbers.

Ruckenstein (Ref. 34).

$$\left. \begin{array}{l} Nu = 0.895(\dfrac{\beta}{Z})^{1/2}\, Pe_h^{1/2} + 2 \\[3mm] Sh = 0.895(\dfrac{\beta}{Z})^{1/2}\, Pe_m^{1/2} + 2 \end{array} \right\} \qquad (2.20)$$

where

$$Z = 2(1 + \beta) \qquad (2.21)$$

$$\beta = \mu_g/(\mu_p + \xi) \qquad (2.22)$$

ξ = "interfacial viscosity" due to adsorbed surfactant impurities.

16

These results apply for moderate to strong internal circulation, large Peclet numbers, and small particle Reynolds numbers.

When the relative velocity between a cloud of droplets and the surrounding fluid approaches zero the following relationship may be used to determine the transfer rates (Ref. 31).

$$\left.\begin{array}{l} Nu = 2/(1 - \sigma_V^{1/3}) \\[2mm] Sh = 2/(1 - \sigma_V^{1/3}) \end{array}\right\} \tag{2.23}$$

The Nusselt and Sherwood numbers are defined in the same manner as for the single droplet case, but note that the fluid surrounding the cloud of particles may well include other particle clouds and therefore the thermal conductivity, thermal diffusivity, and binary diffusion coefficient must be modified accordingly.

The interfacial convective heat (or mass) transfer between a cloud of droplets and the surrounding fluid is not only a function of the Péclét number (Pe_h, Pe_m) and the internal circulation of the particles. It is also a function of particle concentration and particle size distribution. These reflect the influence of both particle-particle interaction and hydrodynamic fluid-particle interaction. References (35-44) provide a short bibliography on this subject. Two examples of correlations are given here, one due to Reference 36 and the other due to Reference 41.

Pfeffer (Ref 36).

$$\left.\begin{array}{l} Nu = 1.26\left[\dfrac{1 - \sigma_V^{5/3}}{Y - \sigma_V^{1/3} X}\right] Pe_h^{1/3} + \dfrac{2}{(1 - \sigma_V^{1/3})} \\[5mm] Sh = 1.26\left[\dfrac{1 - \sigma_V^{5/3}}{Y - \sigma_V^{1/3} X}\right] Pe_m^{1/3} + \dfrac{2}{(1 - \sigma_V^{1/3})} \end{array}\right\} \tag{2.24}$$

17

where

$$Y = 2 + 2\beta + \sigma_V^{5/3}(3 - 2\beta) \tag{2.25}$$

$$X = 3 + 2\beta + 2\sigma_V^{5/3}(1 - \beta). \tag{2.26}$$

Note that the relative velocity used to define the cloud Péclét number is defined as the difference between the gas flow velocity and the mean velocity assigned to the cloud of particles. Refer to the second consideration listed in Section 2.

Pfeifer's results apply to the flow of an ensemble of uniform size particles with no internal circulation, a large Péclét number, and a small particle Reynolds number.

Yaron and Gal-or (Ref. 41)

$$Nu = \frac{1.1284 \ Pe_h^{1/2}}{(1 - \sigma_V)^{1/2}} \ [1 - \frac{2.8852}{Re_p^{1/2}} \ F(\mu,\rho)] + \frac{2}{(1 - \sigma_V^{1/3})} \tag{2.27}$$

$$Sh = \frac{1.1284 \ Pe_h^{1/2}}{(1 - \sigma_V)^{1/2}} \ [1 - \frac{2.8852}{Re_p^{1/2}} \ F(\mu,\rho)] + \frac{2}{(1 - \sigma_V^{1/3})} \tag{2.28}$$

where $\qquad F(\mu,\rho) = [1 + \frac{1.5}{\beta}]/[1 + (\frac{\rho_p \ \mu_p}{\rho_g \ \mu_g})^{1/2}].$

These results apply to the flow of a cloud of uniform size particles with no restriction on the amount of internal circulation, a large Péclét number, and $50 \leq Re_p \leq 1500$.

As previously mentioned, we are interested in the variation of the thermal conductivity of the overall mixture with particulate volume fraction, σ_V. Gotoh, Reference 45, recommends without restrictions the use of the following equation for evaluating the effective thermal conductivity of two-phase heterogeneous flow.

18

$$1 - \sigma_v = [\frac{k_p - k_e}{k_p - k_g}][\frac{k_g}{k_e}] \qquad (2.29)$$

where

k_e = the effective thermal conductivity of the mixture.

Yamada and Takahashi, Reference 46, have conducted an interesting study on the variation of the effective thermal conductivity of suspensions with particle shape, orientation, dimension, and surface condition.

3. PERFORMANCE ESTIMATION

In light of the discussion in Section 2, a multi-stage axial compressor operating with a two-phase fluid is studied best by dividing it into three parts as follows:

1) The low pressure stages in which no substantial change of phase (from liquid to vapor) has occured;

2) The intermediate stages in which there is a complete change of phase; and

3) The high pressure stages in which one has essentially an air-vapor mixture.

In each group there is a change of performance, efficiency, and surge margin.

In view of the uncertainties on transport properties of particulate two-phase flow, we have concentrated in the present investigation on the performance of a compressor operating with air-vapor mixture. This effort is divided into the following:

(1) Performance calculation of a single stage air compressor, PURDUE 001 & 002 Compressors

(2) Performance calculation for the multi-stage compressor, N.G.T.E. #109 Compressor

(3) Performance calculation for the P&W TF-30 Compressor.

Each of the forementioned are evaluated using temperatures corresponding to: (1) design conditions - 288 K, (2) air containing water vapor in the form of dry steam - 373 K, and (3) air before the latent heat is absorbed due to evaporation - 429.04 K or 484.79 K.

20

3.1 Single Stage Compressor

A single stage compressor was desinged with the following design parameters:

mass flow	=	20 kg/sec
stage temperature rise	=	20°C
r.p.m.	=	9,000
mean blade speed	=	180 m/sec

Both a constant reaction (PURDUE 001) and a free-vortex (PURDUE C02) compressors were designed.

The performance of the single stage compressor was calculated for operation with the following working fluids:

a) air at 14.70 psia pressure and 429.04°K, 373.0°K, and 288.0°K temperature.

b) air mixed with 5.0% steam (by weight) at 14.70 psia and 373.0°K temperature. The results are presented in Figs. 3.1-3.13.

3.2 Multistage Compressor: N.G.T.E. #109

The design details for this compressor can be found in Ref. 47.

The performance of the compressor was calculated for operation with the following working fluids:

(a) air at 14.70 psia pressure and 484.79°K

(b) air mixed with 10% steam (by weight) at 14.70 psia pressure and 373.0°K temperature

The results are presented in Fig. 3.14.

21

3.3 P&W TF-30 Compressor

In view of the lack of consistent design and experimental data, it has not been possible to carry out performance calculations, although plans have been made to carry out the following calculati.ns:

(a) H.P. compressor performance with air mixed with 10% by weight steam.

(b) L.P. compressor performance in the initial stages with air mixed with 10% by weight water in uniform droplet form.

(c) Stage 10 with sudden evaporation of 5% water and with air mixed with 10% by weight steam, although this is in principle equivalent to the calculation described under 3.1.

4. COMPRESSOR AEROTHERMODYNAMICS

The compressor aerothermodynamics developed here is based on References 48-56. However, the working fluid is assumed to be an air-water mixture in which there can arise a change of phase from liquid water to vapor. In view of the fact that the water droplets may be subjected to gravitational forces, especially in inter-blade spacings and in non-rotating blade passages, gravitational forces have been included in the three-dimensional two-phase flow equations.

In the absence of gravitational forces, it is proposed to develop a compressor performance calculation method based on the axisymmetric flow assumption.

4.1 General Considerations

a) State Relations

i) GAS PHASE: The gas phase is considered to be a mixture of air and water vapor that behaves as a perfect gas. Therefore,

$$P_g = \rho_g R_g T_g \tag{4.1}$$

where

P_g = pressure associated with the gas phase

R_g = gas phase gas constant.

ii) LIQUID PHASE: The liquid phase is assumed to have a constant density,

$$\rho_p = 0.988 \text{ gm/cm}^3. \tag{4.2}$$

It is assumed that when σ_v reaches a value of 0.40 for tap water and air (0.90 for "pure" water and air) at a pressure of one atmosphere a film arises on the casing wall (Section 2.5).

23

b) Stress-Strain Relations

i) Pressure: The mixture pressure (gas continuum + liquid "continuum") is assumed to be equal to the gas phase pressure, P_g. It is assumed that the water droplets do not contribute to the local pressure due to the lack of randomness in local particle motion.

ii) Viscosity: A turbulent, isotropic, effective coefficient of viscosity based on gas-phase Reynolds number is assumed throughout. The water droplet content is therefore not accounted for in estimating the mixture viscosity.

iii) Viscous force on droplets: The viscous force on droplets is based on a Reynolds number calculated with respect to the gas phase kinematic viscosity (effective), the relative gas velocity, and the local statistical mean diameter of the droplet (Section 2.6).

iv) Surface tension: The droplet breakup is based upon a critical value of Weber number (of the order of ten) and the surface tension for water is taken to be

$$\sigma = 67.91 \text{ dynes/cm.} \tag{4.3}$$

c) Water Droplet Fraction

The particulate droplet mass fraction is defined as follows:

$$\sigma_m = (m_p/Vol_{\bar{m}})/(m_{\bar{m}}/Vol_{\bar{m}}) = \frac{m_p}{m_{\bar{m}}} \tag{4.4}$$

where

σ_m = particulate droplet mass fraction

m = mass

Vol = Volume

$(\ )_{\bar{m}}$ = pertaining to the mixture as a whole.

24

The particulate droplet volume fraction is defined as follows:

$$\sigma_v = Vol_p/Vol_{\bar{m}} \ . \tag{4.5}$$

Expanding Equation (4.4) and substituting (4.5) an expression is obtained relating σ_v and σ_m

$$\sigma_m = \sigma_v \, \rho_p/(\sigma_v[\rho_p - \rho_g] + \rho_g) \tag{4.6}$$

or

$$\sigma_v = \sigma_m \, \rho_g/(\rho_p - \sigma_m[\rho_p - \rho_g]). \tag{4.7}$$

σ_v is a function of the statistical mean diameter and number density of the particulate cloud.

$$\sigma_v = \frac{\pi}{6} \, d_s^3 \, N_s \tag{4.8}$$

where again

d_s = the Sauter statistical mean diameter of a cloud of droplets

N_s = the statistical number density, i.e. the statistical number of d_s size particles per unit volume of overall mixture.

4.2 Conservation Equations

a) Assumptions

i) The gas phase is assumed to be a perfect gas continuum.

ii) The particulate liquid phase is assumed to be a continuum that does not contribute to the local pressure. Two exceptions to this continuum assumption are the determination of a) the viscous interaction force between the particulate liquid and gas phases, and (b) the interfacial heat and mass transfers.

25

iii) Mass conservation is assumed for each of the two phases, the gas phase and the particulate liquid phase, allowing for phase change.

iv) The liquid mass that is vaporized is assumed to be instantly and intimately mixed with the gas phase, i.e. large scale vapor concentration gradients and the momentum of the vaporized mass are neglected.

v) On the scale of droplet dimensions, there are local variations in velocity, temperature, and vapor concentration. The evaporation of individual droplets is calculated as a process dependent upon such local properties.

vi) When axial symmetry of the flow is assumed, it is necessary to treat the gravitational body force as being negligible.

b) Description of Coordinate Systems

The equations have been deduced using two coordinate systems, intrinsic and cylindrical.

i) Intrinsic Coordinate System (Figure 4.1)

The m, θ, n intrinsic system is a local, right hand, orthogonal system. The m-direction lies tangent to the local streamline direction, and the θ-direction is orthogonal to the m-r plane where r is the radial vector defined in Figure 4.1. The n-direction is normal to the m-direction in the local meridional plane.

ii) Cylindrical Coordinate System (Figure 4.2)

The cylindrical system is fixed to the axis of rotation of the compressor. The z-direction lies along the axis of rotation

26

in the direction of the bulk flow and r is in the radial direction. The θ-component is in the circumferential direction defined positive with respect to a right-hand r,θ,z orthogonal coordinate system.

iii) Rotation of the Machine

It is more convenient to work in coordinate systems which are stationary with respect to a rotating blade row. Hence fluid velocities for a rotating machine are defined as follows:

(1) Intrinsic Coordinates

$$\bar{V} = \bar{W} + \bar{U} \tag{4.9}$$

where

$\bar{V}$ = absolute velocity vector

$\bar{W}$ = relative velocity vector

$\bar{U}$ = local blade rotational velocity vector = $\bar{U}_m + \bar{U}_\theta + \bar{U}_n$

$\bar{U}_m, \bar{U}_\theta, \bar{U}_n$ = the m,θ,n components of $\bar{U}$, respectively,

but

$$\left.\begin{array}{l} U_m = f_m(U,\phi_1,\phi_2) \\[2mm] U_\theta = f_\theta(U,\phi_1,\phi_2) \\[2mm] U_n = f_n(U,\phi_1,\phi_2) \end{array}\right\} \tag{4.10}$$

where

U = the magnitude of the local blade rotational velocity vector

U_m, U_θ, U_n = the magnitudes of the m,θ,n components of $\bar{U}$

ϕ_1 = the angle between the radius vector and the m-direction

ϕ_2 = the angle between the radius vector and the n-direction.

27

Therefore,

$$
\left.\begin{array}{ll}
V_{gm} = W_{gm} + U_m & V_{pm} = W_{pm} + U_m \\[2mm]
V_{g\theta} = W_{g\theta} + U_\theta & V_{p\theta} = W_{p\theta} + U_\theta \\[2mm]
V_{gn} = W_{gn} + U_n = 0 & V_{pn} = W_{pn} + U_n = 0
\end{array}\right\} \tag{4.11}
$$

(2) Cylindrical Coordinates

Again

$$
\bar{V} = \bar{W} + \bar{U},
$$

where similarly

$$
\bar{U} = \bar{U}_r + \bar{U}_\theta + \bar{U}_z. \tag{4.12}
$$

But

$$
\bar{U}_r = \bar{U}_z = 0. \tag{4.13}
$$

Therefore

$$
\bar{U} = \bar{U}_\theta \tag{4.14}
$$

and

$$
U = U_\theta = r\omega \tag{4.15}
$$

where

ω = angular velocity of the rotating blade row.

As a result,

$$
\left.\begin{array}{ll}
V_{gr} = W_{gr} & V_{pr} = W_{pr} \\[2mm]
V_{g\theta} = W_{g\theta} + r\omega & V_{p\theta} = W_{p\theta} + r\omega \\[2mm]
V_{gz} = W_{gz} & V_{pz} = W_{pz}
\end{array}\right\} \tag{4.16}
$$

c) Flow Equations

The following flow equations are deduced in both sets of
coordinate systems for three-dimensional as well as axisymmetric
flow. They consist of the following:

28

i) Mass Conservation equations

ii) Momentum Conservation equations

iii) Energy Conservation equations

iv) Variation of σ_v with respect to the three coordinate directions

v) Radial Equilibrium equations

The equations are presented in Appendix II as follows.

II.1. Three-dimensional Flow Equations in Intrinsic Coordinates

II.2. Axisymmetric Flow Equations in Intrinsic Coordinates

II.3. Three-dimensional Flow Equations in Cylindrical Coordinates

II.4. Axisymmetric Flow Equations in Cylindrical Coordinates

5. DISCUSSION

The study presented in this Report is concerned with the operation of an aircraft compressor with an air-water mixture ingested into the engine either from puddles on runways or from rain at altitude.

The water in the air-water mixture may be found in several states (discrete droplets, film of water, evaporating droplets and steam) between the inlet and outlet of a large pressure ratio multi-stage machine, such as the TF-30 compressor. Agglomeration and break-up of droplets, the transport processes (mass and heat) between the droplets and the surrounding air and the drag of droplets are not phenomena that are well understood quantitatively. They are central to gaining an understanding of the changes in the state of water in the system.

The presence of water in air also affects the compressibility of the mixture and therefore the local Mach number at any location in the compressor becomes a function of the state and content of water in the mixture.

The rotating flow field of a compressor has a strong influence on the state and distribution of water since centrifugal forces and Coriolis forces affect both discrete droplets and films of water.

Discrete droplets are also subject to gravitational influence, at least at low rotating speeds and in inter-row spacings and stators.

In examining the performance of a multi-stage compressor with an air-water mixture flow, it seems most useful to divide the compressor into groups of stages on the basis of the state in which water is expected to be found in each group. In doing this, there arise at least two important uncertainties: (1) the formation of a film at the casing wall and (2) the gradual evaporation of the droplets.

30

Some preliminary investigations conducted on the performance of a single stage machine with air-water droplet mixture flow have revealed that the water droplets cause both a reduction in mass flow as well as a slight change in efficiency, mainly due to incidence and Mach number effects.

The performance of stages where the droplets are expected to be evaporating cannot be estimated with any degree of accuracy based on overall stage characteristics. Nevertheless, it is possible to argue that the stages where the largest amount of evaporation occurs must show the largest change in performance on account of the sudden fall in air temperature due to latent heat absorption by the water.

When there is an air-steam mixture flow, it is possible to make a rough estimate of the change in overall stage characteristics. It is found, both in a single stage compressor and in a multi-stage machine, that there is a noticeable deterioration in performance both in efficiency as well as in the surgeline.

In order to perform more satisfactory calculations, it is imperative that one proceeds to set up the equations of aerothermodynamics for air-water mixture flow in a compressor. This task has been completed both in general three-dimensional coordinates as well as in axisymmetric coordinates. Such equations involve several quantities that can only be estimated very roughly and hence can perhaps be treated only in a parametric form: (1) volume fraction of the water droplets, (2) statistical mean diameter and number density of droplets, (3) mass, momentum and energy transfer between the droplets and the air, and (4) degree of mixing between evaporated water and the surrounding air.

31

The equations for air-water mixture, when compared with the standard compressor flow equations for air flow, reveal several ways in which computational programs set up for air flow can be adapted for use with air-water mixture flow.

In examining the problem from the point of view of alleviating the effects of water ingestion, one can arrive at several methods of attack on the problem:

(a) Removal of as much water as possible at the casing walls.

(b) Bleed-in of air into the latter stages of the compressor from another stream.

(c) Variable geometry engine with adjustable air flow paths.

5.1. Recommendations

The recommendations may be divided broadly into two categories:

(i) Further diagnostic studies.

(ii) Future studies.

5.1.1. Further diagnostic studies

(1) Estimation of performance of selected multi-stage machines (incorporating bleed-in and bleed-out) on the basis of stage characteristics when there is a simultaneous change in temperature from the design value and an addition of steam.

(2) Estimation of the effect of bypass ratio on the performance of compressors with two-phase flow.

(3) Study of two-phase flow in a diffusing passage.

(4) Adaptation of simple, existing computational programs for air flow to air-water mixture flow on the basis of parameterized droplet dynamics and transport processes for the study of a selected multi-stage machine.

32

(5) A flow visualization study on a multi-stage compressor to establish the water droplet dynamics when water is ingested into the air stream at entry to the compressor

(6) A flow visualization study on a multi-stage compressor with selected inlet configurations to establish the water droplet dynamics when water is injected into the air stream at entry to the inlet.

(7) A flow visualization study on a rotating tire in a wind tunnel equipped with a moving belt floor to establish the influence of a few selected tire parameters on the jet created by the motion of the tire.

5.1.2. Future studies

(1) Development of a comprehensive computational program for air-water mixture flow through an axial compressor with appropriate droplet dynamics and transport coefficients.

(2) Analysis of the performance of compressors using the computational program developed to establish the scope and implications of variable cycle/geometry schemes.

(3)(a) Study of bleed-out of water in early stages.

(b) Study of bleed-in of air into the latter stages.

(4) Determination of classes of compressors to which different classes of controls can be applied.

(5) Study of the effects of engine-airframe integration parameters on the utilization of different kinds of controls.

(6) Study of the water jet created by a moving aircraft tire on a wet runway in relation to the location of the engine inlet.

(7) Determination of the effect of water vapor on after-burner stability, particularly in relation to the fuel vaporization and combustion characteristics.

33

6. LIST OF REFERENCES

1. Willenborg, J. A., Jordan, J. E., Schumacher, P. W. J., Hughes, P. L., Willocks, H. J., Crabtree, C. F., Shafer, R., Connell, R. E., Dean, R., Scott, D. L., and Stibich, M. A., "F-111 Engine Water Ingestion Review," F-111 System Program Office, Wright-Patterson Air Force Base, Dayton, Ohio, October 31-November 10, 1972.

2. Holmboe, J., Forsythe, G. E., and Gustin, W., Dynamic Meterology, pp. 57-60, John Wiley and Sons, Inc., New York, 1945.

3. Green, H.L. and Lane, W. R., Particulate Clouds, Spon Ltd., London, 1964.

4. Fuchs, N. A., The Mechanics of Aerosols, Pergamon Press, Ltd., London, 1964.

5. Soo, S. L., Fluid Dynamics of Multiphase Systems, Blaisdell Publishing Company, Waltham, Massachusetts, 1967.

6. Wallis, G. B., One-dimensional Two-phase Flow, McGraw-Hill, Inc., U.S.A., 1969.

7. Rudinger, G., "Fundamentals and Applications of Gas-Particle Flow," Paper prepared for the meeting of the AGARD Fluid Dynamics Panel in Rome, Italy, September, 1974.

8. Briggs, J., "Probabilities of Aircraft Encounters with Heavy Rain," Meterological Magazine, Vol. 101, pp. 8-13, 1972.

9. Methven, T. J. and Fairheed, B., "A Correlation between Rain Erosion of Perspex Specimens in Flight and on a Ground Rig," A.R.C. Technical Report 21,090, C.P. No. 496, 1960.

10. Hays, D. and Browne, A. L., Ed., "Symposium on the Physics of Tire Traction," General Motors Corporation Research Laboratories, Plenum Press, New York, 1974.

11. Collier, J. G. and Wallis, G. B., Two-phase Flow and Heat Transfer, Vol. II, pg. 405, Dept. of Mechanical Engineering, Stanford University, Stanford, California, 1967.

12. Wallis, G. B., One-dimensional Two-phase Flow, pp. 378-380, McGraw-Hill, Inc., U.S.A., 1969.

13. Ibid, pp. 376-377.

14. Ibid, pp. 265-267.

15. Swain, C. E., "The Effect of Particle/Shock Layer Interaction on Re-entry Vehicle Performance," AIAA Paper 75-734, June, 1975.

16. Ergun, S., "Fluid Flow through Packed Columns," Chemical Engineering Progress, Vol. 48, No. 2, pp. 89-94, February, 1952.

17. Ingebo, R. D., "Drag Coefficients for Droplets and Solid Spheres in Clouds Accelerating in Airstreams," NACA Technical Note 3762, May, 1956.

18. Marble, F. E., "Mechanism of Particle Collision in the One-dimensional Dynamics of Gas-Particle Mixtures," The Physics of Fluids, Vol. 7, No. 8, pp. 1270-1282, August, 1964.

19. Fuchs, N. A., The Mechanics of Aerosols, pp. 21-159, Pergamon Press, Ltd., London, 1964.

20. Soo, S. L., "Dynamics of Multiphase Flow Systems," Industrial and Engineering Chemistry Fundamentals, Vol. 4, No. 4, pp. 426-433, November, 1965.

21. Soo, S. L., Fluid Dynamics of Multiphase Systems, pp. 185-244, Blaisdell Publishing Company, Waltham, Massachusetts, 1967.

22. Tam, C. K. W., "The Drag on a Cloud of Spherical Particles in Low Reynolds Number Flow," Journal of Fluid Mechanics, Vol. 38, Part 3, pp. 537-546, 1969.

23. Rudinger, G., "Effective Drag Coefficient for Gas-Particle Flow in Shock Tubes," Journal of Basic Engineering, Transactions of the ASME, Series D, Vol. 92, pp. 165-172, March, 1970.

24. Pai, S. I. and Hsieh, T., "Interaction Terms in Gas-Solid Two-phase Flows," Zeitschrift Fur Flugwissen Schaften, Vol. 21, Heft 12, pp. 442-445, 1973.

25. Rudinger, G., "Fundamentals and Applications of Gas-Particle Flow," pp. 12-14, Paper prepared for the meeting of the AGARD Fluid Dynamics Panel in Rome, Italy, September, 1974.

26. Hamed, A. and Tabakoff, W., "Solid Particle Demixing in a Suspension Flow of Viscous Gas," Journal of Fluids Engineering, Transactions of the ASME, Series I, Vol. 97, No. 1, pg. 106-111, March, 1975.

27. Law, C. K., "A Theory for Monodisperse Spray Vaporization in Adiabatic and Isothermal Systems," International Journal of Heat and Mass Transfer, Vol. 18, pp. 1285-1292, 1975.

28. Batchelor, G. K., "Brownian Diffision of Particles with Hydrodynamic Interaction," Journal of Fluid Mechanics, Vol. 74, No. 1, pp. 1-29, 1976.

29. Rudinger, G., "Fundamentals and Applications of Gas-Particle Flow," pp. 14-15, Paper prepared for the meeting of the AGARD Fluid Dynamics Panel in Rome, Italy, September, 1974.

30. Griffith, R. M., "Mass Transfer from Drops and Bubbles," Chemical Engineering Science, Vol. 12, pp. 198-213, 1960.

31. Yaron, I. and Gal-or, B., "Convective Mass or Heat Transfer from Size-distributed Drops, Bubbles, or Solid Particles," International Journal of Heat and Mass Transfer, Vol. 14, pp. 727-737, 1971.

32. Friedlander, S. K., "Mass and Heat Transfer to Single Spheres and Cylinders at Low Reynolds Numbers," _American Institute of Chemical Engineers Journal_, Vol. 3, pg. 43, 1957.

33. Levich, V., _Physiochemical Hydrodynamics_, Prentice-Hall, Englewood Cliffs, New Jersey, 1962.

34. Ruckenstein, E., "On Mass Transfer in the Continuous Phase from Spherical Bubbles or Drops," _Chemical Engineering Science_, Vol. 19, pg. 131, 1964.

35. Hsu, N. T., Sato, K., and Sage, B. H., "Material Transfer in Turbulent Gas Streams," _Industrial and Engineering Chemistry_, Vol. 46, No. 5, pp. 870-876, May 1954.

36. Pfeffer, R., "Heat and Mass Transport in Multiparticle Systems," _Industrial and Engineering Chemistry Fundamentals_, Vol. 3, No. 4, November, 1964.

37. Kunii, Daizo and Suzuki, Motoyuki, "Particle-to-Fluid Heat and Mass Transfer in Packed Beds of Fine Particles," _International and Journal of Heat and Mass Transfer_, Vol. 10, pp. 845-952, 1967.

38. Gal-or, B. and Walatka, V., "A Theoretical Analysis of Some Interrelationships and Mechanisms of Heat and Mass Transfer in Dispersions," _American Institute of Chemical Engineers Journal_, Vol. 13, No. 4, pp. 650-657, July, 1967.

39. Gal-or, B., "Coupled Heat and Multicomponent Mass Transfer in Particulate Systems with Residence Time and Size Distributions," _International Journal of Heat and Mass Transfer_, Vol. 11, pp. 551-565, 1968.

40. Waslo, S. and Gal-or, B., "Boundary Layer Theory for Mass and Heat Transfer in Clouds of Moving Drops, Bubbles, or So. i Particles," Chemical Engineering Science, Vol. 26, pp. 829-838, 1971.

41. Yaron, I. and Gal-or, B., "High Reynolds Number Fluid Dynamics and Heat and Mass Transfer in Real Concentrated Particulate Two-phase Systems," International Journal of Heat and Mass Transfer, Vol. 16, pp. 887-895, 1973.

42. Hughmark, G. A., "Heat Transfer in a Fluidized Bed of Small Particles," American Institute of Chemical Engineers Journal, Vol. 19, No. 3, pp. 658-659, May, 1973.

43. Yaron, I. and Gal-or, B., "Low Péclét Number Mass or Heat Transfer in Two-phase Particulate Systems," American Institute of Chemical Engineers, Vol. 19, No. 3, pp. 662-664, May, 1973.

44. Labowsky, M., "The Effects of Nearest Neighbor Interaction on the Evaporation Rate of Cloud Particles," Engineering and Applied Science Dept., Yale University, New Haven, Connecticut, August, 1975.

45. Gotoh, K., "Thermal Conductivity of Two-phase Heterogeneous Substances," International Journal of Heat and Mass Transfer, Vol. 14, pp. 645-646, 1971.

46. Yamada, E. and Takahashi, K., "Effective Thermal Conductivity of Suspensions - 1st Report: Analysis of the Effects of Various Factors by the Electrolytic-Bath Method," Heat Transfer - Japanese Research, Cosponsored by The Society of Chemical Engineers of Japan and The Heat Transfer Division of ASME, Vol. 4, No. 1, January-March, 1975.

47. Carter, A. D. S., Turner, R. C., Sparkes, D. W., and Burrows, R. A., "The Design and Testing of an Axial-Flow Compressor having Different Blade Profiles in Each Stage," Communicated by the Director-General of Scientific Research (Air), Ministry of Supply, Reports and Memoranda No. 3183, November, 1957.

48. Shapiro, A. H., The Dynamics and Thermodynamics of Compressible Fluid Flow, Vol. I and II, The Ronald Press Company, New York, 1953.

49. Schlichting, H., Boundary Layer Theory, Pergamon Press, Ltd., New York, 1955.

50. Oswatitsch, Klaus, Gas Dynamics, Academic Press, Inc., New York, 1956.

51. Emmons, H. W., Fundamentals of Gas Dynamics, Princeton University Press, New Jersey, 1958.

52. Daily, J. W. and Harleman, D. R. F., Fluid Dynamics, Addison-Wesley Publishing Company, Inc., Reading, Massachusetts, 1966.

53. Wooten, D. C., "The Attenuation and Dispersion of Sound in a Condensing Medium," Ph.D. Thesis, California Institute of Technology, Pasadena, California, 1967.

54. Marble, F. E., "Dynamics of Dusty Gases," Annual Review of Fluid Dynamics, pp. 397-445, Annual Reviews, Inc., 1970.

55. Sonntag, R. E. and Van Wylen, G. J., Introduction to Thermodynamics: Classical and Statistical, John Wiley and Sons, Inc., New York, 1971.

56. Wennerstrom, A. J., "On the Treatment of Body Forces in the Radial Equilibrium Equation of Turbomachinery," ARL 75-0052, April, 1974.

57. Lighthill, M. J., "Mathematics and Aeronautics," Journal of the Royal Aeronautical Society, Vol. 64, No. 595, pp. 375-394, July, 1960.

58. Taylor, G. I., "Generation of Ripples by Wind Blowing over a Viscous Fluid," The Scientific Papers of G. I. Taylor, ed., G. K. Batchelor, Vol. 3, pp. 244-254, Cambridge University Press, 1963.

39

FIGURES

FIGURE 2.1

VELOCITY OF SOUND
vs
LIQUID VOLUME FRACTION
(At Standard Atmospheric Conditions)

41

FIGURE 3.1a

PURDUE OGI COMPRESSOR - CONSTANT REACTION
Pressure Ratio v.s. Mass Flow

KEY

100% Air at 429.04K

95% Air + 5% Steam at 373K

Blade Tip Values

RPM = 9900

PRESSURE RATIO, P_{0_2}/P_{0_1}

NON-DIMENSIONAL MASS FLOW, $\dfrac{\dot{m}\sqrt{T_0}}{P_0}\sqrt{\dfrac{1}{m.w.}}$

PURDUE 001 COMPRESSOR – CONSTANT REACTION
Efficiency v.s. Mass Flow

RPM = 9900

9900

3600

KEY

—— 100% Air at 429.04K

—— 95% Air + 5% Steam at 373K

Blade Tip Values

EFFICIENCY, η

NON-DIMENSIONAL MASS FLOW, $\dfrac{\dot{m}\sqrt{T_0}}{P_0}\sqrt{\dfrac{1}{\gamma\,m_i\,w\cdot\gamma_i}}$

FIGURE 3.1b

43

PURDUE 002 COMPRESSOR - FREE VORTEX
Pressure Ratio v.s. Mass Flow

KEY

100% Air at 429.04K

95% Air + 5% Steam at 373K

Blade Tip Values

RPM = 9900

FIGURE 3.2a

44

PURDUE 002 COMPRESSOR - FREE VORTEX
Efficiency v.s. Mass Flow

RPM = 9900.

9900.

3600.

KEY
100% Air at 429.04K
95% Air + 5% Steam at 373K
Blade Tip Values

NON-DIMENSIONAL MASS FLOW, $\frac{\dot{m}\sqrt{T_0}}{P_0}$, $\sqrt{\frac{T}{m.w}}$, Y

EFFICIENCY, n

FIGURE 3.2b

45

PURDUE OOJ COMPRESSOR - CONSTANT REACTION
Pressure Ratio v.s. Mass Flow

KEY

$-\cdot-$ 100% Air at 288K

$-$ 100% Air at 373K

$-\cdot-$ 95% Air + 5% Steam at 373K

Blade Tip Values

RPM = 9900

NON-DIMENSIONAL MASS FLOW $\dfrac{\dot{m}\sqrt{T_0}}{P_0}\sqrt{\dfrac{\mathbb{T}}{v \cdot m \cdot w \cdot \gamma}}$

PRESSURE RATIO, P_{c_2}/P_{0_1}

FIGURE 3.3a

46

PURDUE 001 COMPRESSOR - CONSTANT REACTION
Efficiency v.s. Mass Flow

Corrected RPM = 2655.1i (RPM = 9900)

2413.7 (9000)

965.5 (3600)

KEY

—— 100% Air at 288K

Blade Tip Values

NON-DIMENSIONAL MASS FLOW $\frac{\dot{m} \sqrt{T_0}}{P_0} \sqrt{\frac{1}{m|w_{\gamma}|Y}}$

EFFICIENCY η

FIGURE 3.3b

47

PURDUE 001 COMPRESSOR - CONSTANT REACTION
Efficiency v.s. Mass Flow

KEY
— — — 100% Air at 373K
— · — 95% Air at 5% Steam at 373K

Blade Tip Values

NON-DIMENSIONAL MASS FLOW, $\frac{\dot{m}\sqrt{T_0}}{P_0}\sqrt{\frac{1}{m \cdot w \cdot \gamma}}$

EFFICIENCY, η

9000 RPM = 9900

3600

FIGURE 3.3c

PURDUE 002 COMPRESSOR - FREE VORTEX
Pressure Ratio v.s. Mass Flow

KEY

100% Air at 288K
100% Air at 373K
95% Air + 5% Steam at 373K

Blade Tip Values

RPM = 9900

FIGURE 3.4a

49

FIGURE 3.4b

PURDUE 002 COMPRESSOR - FREE VORTEX
Efficiency v.s. Mass Flow

EFFICIENCY, η

NON-DIMENSIONAL MASS FLOW $\dfrac{\dot{m}\sqrt{Td}}{P_0} \sqrt{\dfrac{1}{m\,w.\,Y}}$

Corrected
RPM = 2655.1
(RPM = 9900)

2413.7
(9000)

965.5
(3600)

KEY

100% Air at 288K

Blade Tip Values

PURDUE 002 COMPRESSOR - FREE VORTEX
Efficiency v.s. Mass Flow

EFFICIENCY, η

RPM = 9900

9000

3600

KEY

100% Air at 373K

95% Air + 5% Steam at 373K

Blade Tip Values

NON-DIMENSIONAL MASS FLOW, $\frac{\dot{m} \sqrt{T0}}{P0} \sqrt{\frac{1}{m.w. \cdot \gamma}}$

FIGURE 3.4c

FIGURE 3.5a

PURDUE 001 COMPRESSOR - CONSTANT REACTION
Pressure Ratio v.s. Mass Flow

KEY

——— 100% Air at 373K

— · — 95% Air + 5% Steam at 3.3K

Blade Tip Values

Corrected
RPM = 2655.1

2655.1
2413.7
2413.7
965.5
1965.5

PRESSURE RATIO, P_{0_2}/P_{0_1}

1.5
1.4
1.3
1.2
1.1
1.0

NON-DIMENSIONAL MASS FLOW, $\frac{\dot{m}\sqrt{T_0}}{P_0}\sqrt{\frac{\bar{R}}{m.w.\cdot\gamma}}$

0   10   20   30   40   50   60   70   80

PURDUE 001 COMPRESSOR - CONSTANT REACTION
Efficiency v.s. Mass Flow

Corrected
RPM = 2655.1

2655.1

2413.7

2413.7

965.5

965.5

KEY

100% Air at 373K

95% Air + 5% Steam at 373K

Blade Tip Values

NON-DIMENSIONAL MASS FLOW, $\frac{m\sqrt{T_0}}{P_{01}}\sqrt{\frac{R}{\gamma}}$, $\frac{1}{m.w.}$

EFFICIENCY, η

FIGURE 3.5b

53

PURDUE 002 COMPRESSOR - FREE VORTEX
Pressure Ratio v.s. Mass Flow

KEY

— 100% Air at 373K

– – 95% Air + 5% Steam at 373K

Blade Tip Values

Corrected

RPM = 2656.

2655.1

2413.7

2413.7

965.5

965.5

PRESSURE RATIO, P_{o_2}/P_{o_1}

1.6 1.5 1.4 1.3 1.2 1.1 1.0

0   10   20   30   40   50   60   70   80

NON-DIMENSIONAL MASS FLOW, $\frac{m \cdot \sqrt{T_{o_1}}}{P_{o_1}}$, $\sqrt{m \cdot w \cdot \gamma}$

FIGURE 3.6a

54

PURDUE OD2 COMPRESSOR - FREE VORTEX
Efficiency v.s. Mass Flow

2413.7 Corrected
RPM = 2655.1

965.5

KEY

———— 100% Air at 373.

–– – 95% Air + 5% Steam at 373K

Blade Tip Values

EFFICIENCY, %

100

90

80

70

60

40

0   10   20   30   40   50   60   70   80

NON-DIMENSIONAL MASS FLOW, $\frac{\dot{m}\sqrt{T_0}}{P_0}\sqrt{\frac{T}{\gamma m.w.}}\cdot Y$

FIGURE 3.6b

55

PURDUE 001 COMPRESSOR - CONSTANT REACTION and PURDUE 002 COMPRESSOR - FREE VORTEX
Pressure Ratio v.s. Mass Flow

KEY

—————— 100% Air at 373K

———— Blade Mean Values

RPM = 9900

9000

3600

PRESSURE RATIO, P_{0_2}/P_{0_1}

1.25

1.20

1.15

1.10

1.05

1.00

NON-DIMENSIONAL MASS FLOW, $\frac{\dot{m}\sqrt{T_0}}{P_0}\sqrt{\frac{T}{m.w.}}\sqrt{\gamma}$

10   20   30   40   50   60   70   80   90   100

FIGURE 3.7a

56

PURDUE 001 COMPRESSOR - CONSTANT REACTION and PURDUE 002 COMPRESSOR - FREE VORTEX

Efficiency v.s. Mass Flow

RPM = 9900

9900

3600

KEY

100% Air at 373K

Blade Mean Values

EFFICIENCY, η

NON-DIMENSIONAL MASS FLOW, $\dfrac{\dot{m}\sqrt{T_0}}{P_0} \sqrt{\dfrac{1}{m;w;\gamma}}$

FIGURE 3.7b

57

PURDUE OD1 COMPRESSOR - CONSTANT REACTION and PURDUE OD2 COMPRESSOR - FREE VORTEX

Pressure Ratio v. s. Mass Flow

KEY

100% Air at 373K

Blade Mean Values.

Corrected
RPM = 2655.1

2413.7

965.5

$\frac{\dot{m} \sqrt{T_0}}{P_0} \sqrt{\frac{1}{m_1 w_1 \gamma}}$

NON-DIMENSIONAL MASS FLOW,

PRESSURE RATIO, P_{0_2}/P_{0_1}

FIGURE 3.8a

58

FIGURE 3.8b

PURDUE 001 COMPRESSOR - CONSTANT REACTION and PURDUE 002 COMPRESSOR - FREE VORTEX

Efficiency v.s. Mass Flow

Corrected RPM = 2655.

2413.7

965.5

KEY

100% Air at 373K

Blade Mean Values

NON-DIMENSIONAL MASS FLOW, $\dot{m} \frac{\sqrt{T_0}}{P_0} \sqrt{\frac{T}{m \cdot w \cdot \gamma}}$

EFFICIENCY, η

FIGURE 3.9

PURDUE 001 COMPRESSOR - CONSTANT REACTION and PURDUE 002 COMPRESSOR - FREE VORTEX
Total Head Loss and Deflection v.s. Incidence

KEY

— — Mean Total Head Loss

— Mean Deflection

MEAN TOTAL HEAD LOSS, $\overline{\omega}/\frac{1}{2}\rho V^2$

MEAN DEFLECTION, ε (Degrees)

INCIDENCE ANGLE, (Degrees)

60

FIGURE 3.10a

PURDUE DOT COMPRESSOR - CONSTANT REACTION
Air Angle v.s. Radius Ratio
(for design conditions)

AIR ANGLE (Degrees)

RADIUS RATIO, r/r_{mean}

61

FIGURE 3.10b

PURDUE 001 COMPRESSOR - CONSTANT REACTION
Air Angle v.s. Radius Ratio
(for 100% Steam at 373K)

AIR ANGLE (Degrees)

RADIUS RATIO, r/r_{mean}

α_2, β_1

α_1, β_2

FIGURE 3.11a

PURDUE 002 COMPRESSOR - FREE VORTEX
Air Angle v.s. Radius Ratio
(for design conditions)

AIR ANGLE (Degrees)

RADIUS RATIO, r/r_{mean}

63

FIGURE 3.11b

PURDUE 002 COMPRESSOR - FREE VORTEX
Air Angle v.s. Radius Ratio
(for 100% Steam at 373K)

FIGURE 3.12
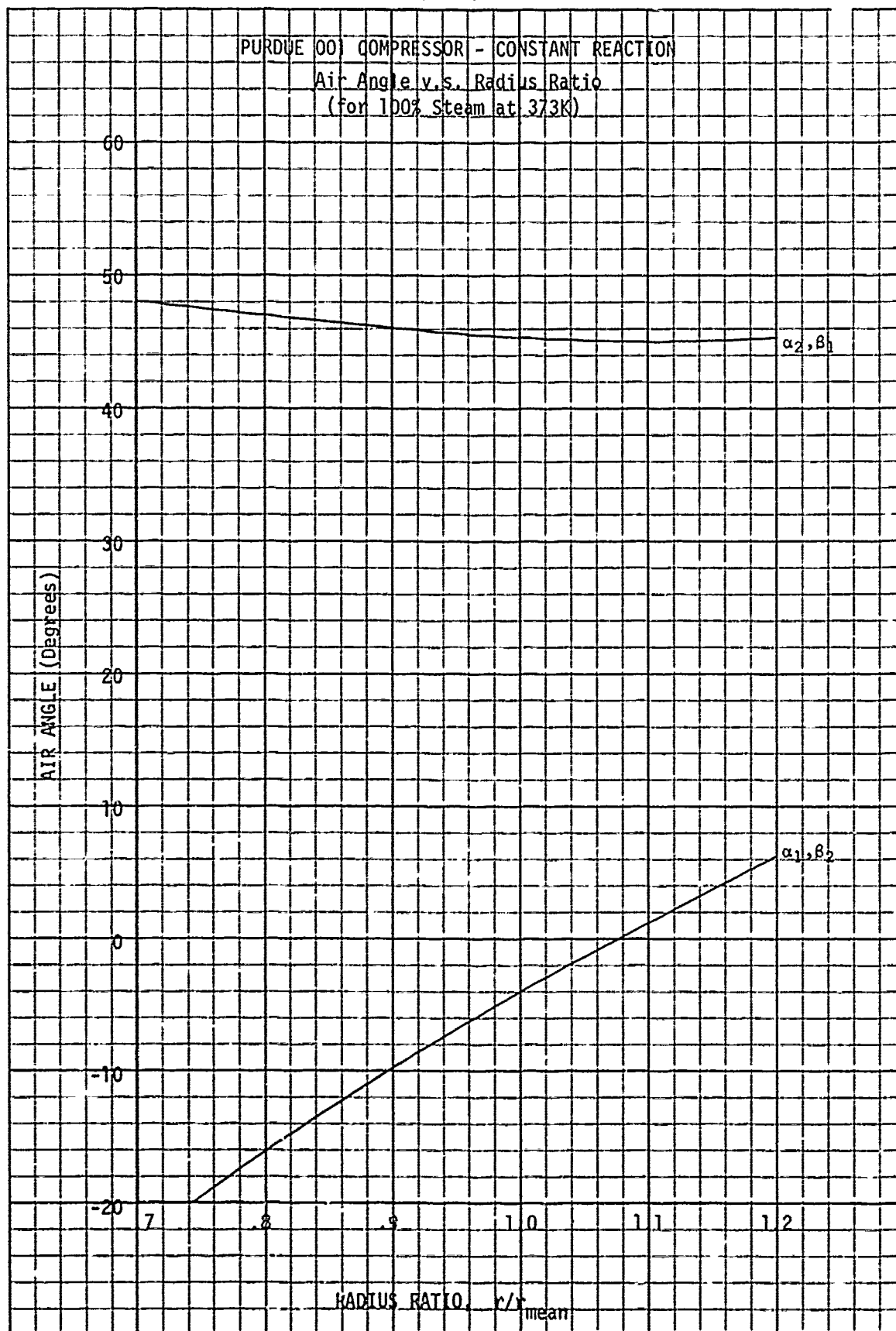
PURDUE 001 COMPRESSOR - CONSTANT REACTION and PURDUE 002 COMPRESSOR - FREE VORTEX

Whirl Velocity v.s. Blade Height

FIGURE 3.13

PURDUE 001 COMPRESSOR - CONSTANT REACTION and PURDUE 002 COMPRESSOR - FREE VORTEX

Whirl Velocity v.s. Blade Height

66

FIGURE 3.14a

FIGURE 3.14a

N.G.T.E. REFERENCE #109 COMPRESSOR
Pressure Ratio v.s. Mass Flow

FIGURE 3.14b

N.G.T.E. REFERENCE #109 COMPRESSOR
Temperature Ratio v.s. Mass Flow

KEY

—— 100% Air at 484.79 K

- - 90% Air + 10% Steam at 373 K

RPM = 9500

RPM = 9500

8000

6000

8000

6000

TEMPERATURE RATIO, T_{O_2}/T_{O_1}

1.8
1.7
1.6
1.5
1.4
1.3
1.2
1.1
1.0

0   50   100   150   200   250

NON-DIMENSIONAL MASS FLOW, $\frac{m \sqrt{T_0}}{P_0} / \sqrt{\frac{1}{m \cdot w \cdot \gamma}}$

68

FIGURE 3.14c

N.G.T.E. REFERENCE #109 COMPRESSOR — 9500 RPM
Stage Efficiency v.s. Mass Flow

STAGE EFFICIENCY, n_{STAGE}

NON-DIMENSIONAL MASS FLOW, $\dfrac{\dot{m}\sqrt{\theta}}{P_0} \bigg/ \sqrt{\dfrac{1}{m \cdot w \cdot \gamma}}$

FIGURE 3.14d

N.G.T.E. REFERENCE #109 COMPRESSOR - 8000 RPM
Stage Efficiency v.s. Mass Flow

NON-DIMENSIONAL MASS FLOW, $\dfrac{m \sqrt{T_0}}{P_0} \sqrt{\dfrac{1}{m.w. \gamma}}$

N.G.T.E. REFERENCE #109 COMPRESSOR - 6000 RPM
Stage Efficiency v.s. Mass Flow

NON-DIMENSIONAL MASS FLOW, $\dfrac{m \sqrt{T_0}}{P_0} \sqrt{\dfrac{1}{m.w. \gamma}}$

70

Three-Dimensional Intrinsic
Coordinate System

Axisymmetric Intrinsic
Coordinate System
Wennerstrom
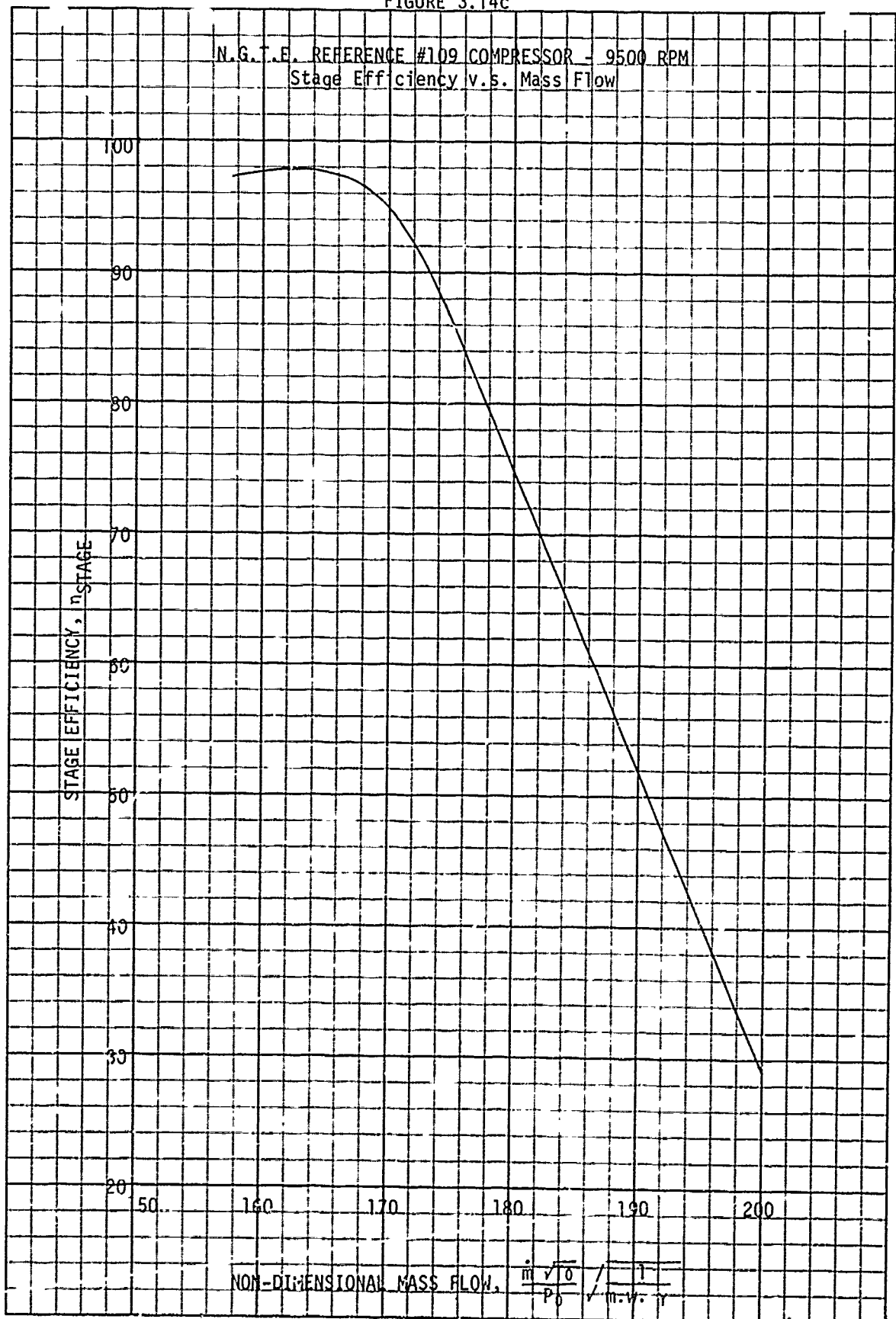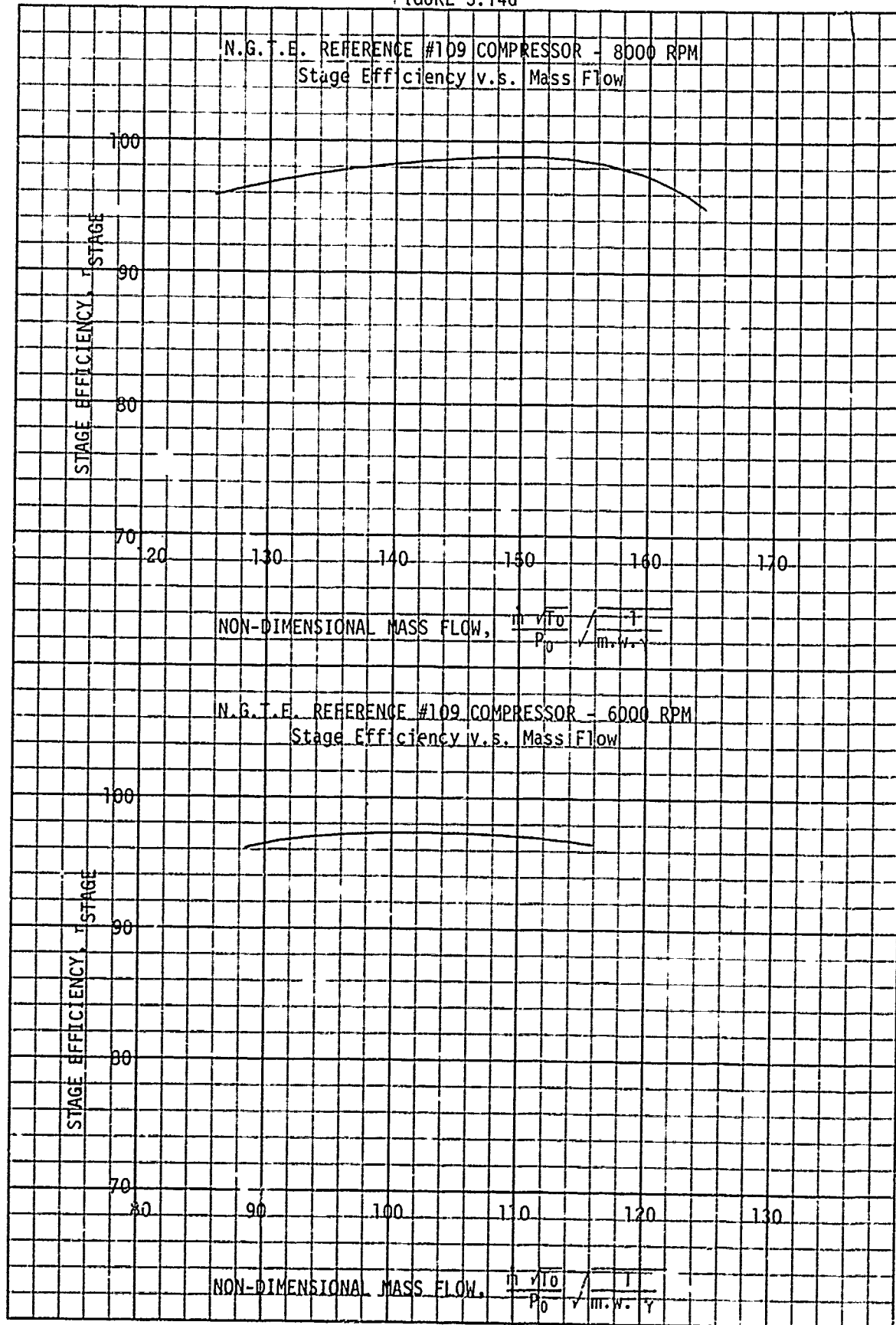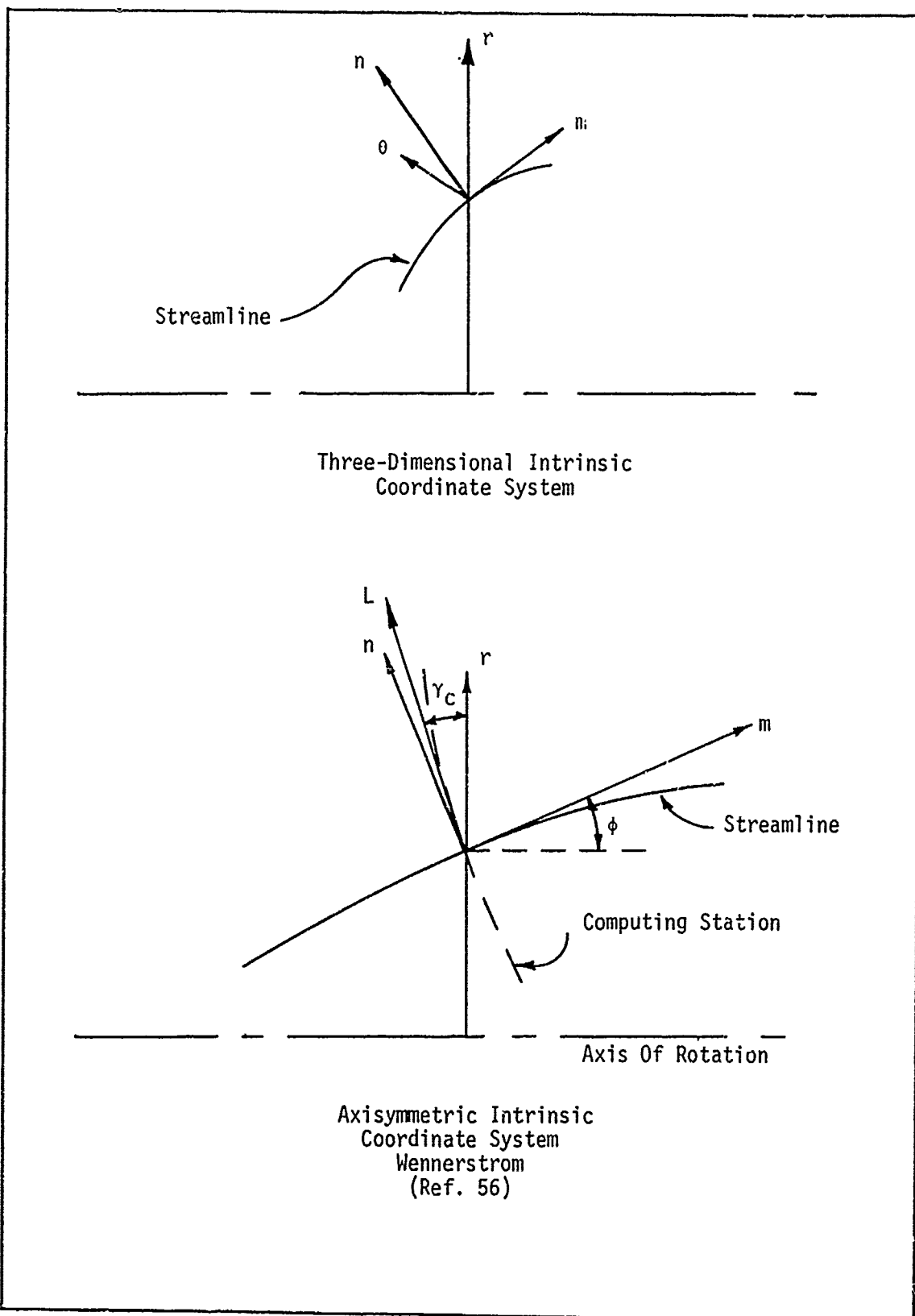(Ref. 56)

FIGURE 4.1

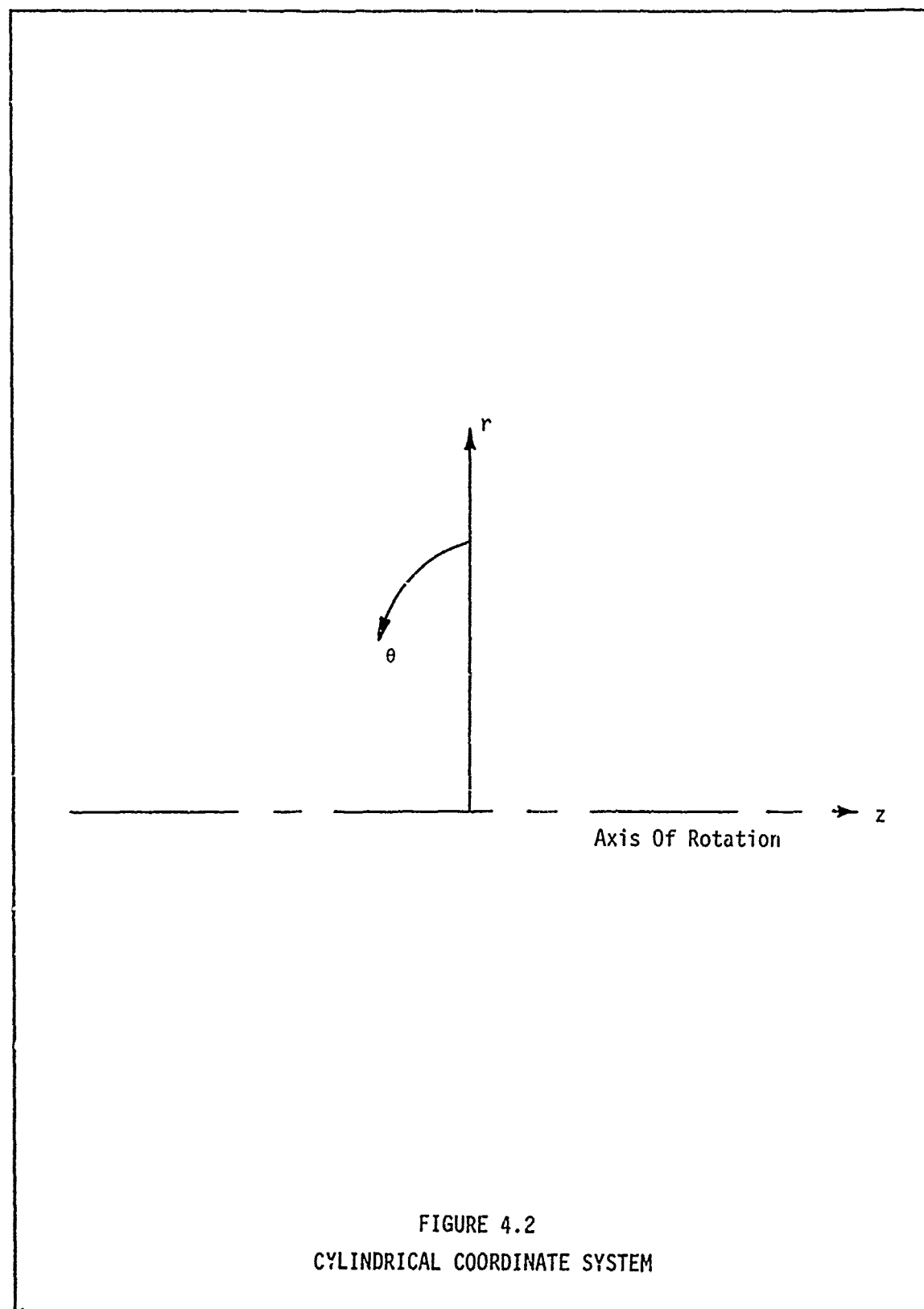INTRINSIC COORDINATE SYSTEM

71

FIGURE 4.2

CYLINDRICAL COORDINATE SYSTEM

APPENDIX I

Estimate of Water Lifted by Wheels

An estimate of the amount of water thrown up by an aircraft wheel from a puddle of depth equal to h can be obtained as follows.

Let the direction of motion of the wheel be x and the transverse direction on the ground be y. Refer to Figure A.I.1.

It has been pointed out (Ref. 57) that the relative flow between the wheel and the water is hypersonic in the sense that the Froude number, $U_c/(g\,h)^{\frac{1}{2}}$, is of the order of 100 when h is of the order of a cm. in depth, and where U_c is the speed of the undercarriage of the wing and hence of the order of tens of meters per second. Accordingly, one can postulate (on the basis of blast wave analogy) a bow wave or hydraulic jump, as shown in Fig. A.I.1, at a distance y_B from the wheel.

Now, a jet of spray can be assumed from the wheel (Ref. 58) on account of the action of the relative wind on the surface of the moving water. The time rate of "pumping" of the water can be written as

$$\dot{m}_W = c_1 \rho_W (\rho_a/\rho_W)^{\frac{1}{2}} \dot{y}_B \tag{A.I.1}$$

where ρ_a is the density of air, ρ_W the density of water, $\dot{y}_B$ the time derivative of y_B, and c_1 a constant equal to approximately one.

In order to obtain $\dot{y}_B$, consider the momentum of the mass, $\rho_W\, y_B\, h$, contained in a strip of water of unit width and the frictional resistance offered by the ground, $f\rho_W\, y_B\, \dot{y}_B^2$, where f is the friction coefficient, of the order of 10^{-2}. The two forces must balance each other together with the momentum loss in the spray. It can then be shown that

$$\dot{y}_B \propto \frac{1}{y_B}\left(1 - n_1 \frac{y_B}{h}\right)^{n_2} \tag{A.I.2}$$

73

where

$$n_1 = 0.5 \, c_1 (\rho_a/\rho_w)^{1/3} \qquad\qquad\qquad \text{(A.I.3)}$$

and

$$n_2 = \frac{n_1 + f}{n_1} \qquad\qquad\qquad\qquad \text{(A.I.4)}$$

Substituting Eq. (A.I.1) into Eq. (A.I.2), the amount of water sprayed behind the wheel per unit distance of wheel travel can be written as follows.

$$m_w = 4\rho_w (\rho_w/\rho_a)^{1/2} \, h^2/c_1. \qquad\qquad \text{(A.I.5)}$$

Thus, the mass of water thrown up from a puddle 0.5 meters long and 2 cm. deep is of the order of 10 kg. during a conventional take-off. This does not yet account for the water sprayed forward of the wheel in its jet stream. During a rain storm, over a runway length of 1,000 meters with a 1 cm. depth of water on the runway, the amount of water lifted off the surface can be as much as several metric tons. Motion pictures of wheel sprays have shown rather large pumping characteristics.

An estimate of the spray envelope from the wheel, y_B and z_B (the height reached by the spray), is rather more difficult to estimate. Some experimental studies on a typical wheel in a moving-belt equipped wind tunnel is indicated before proceeding too far in the analysis.
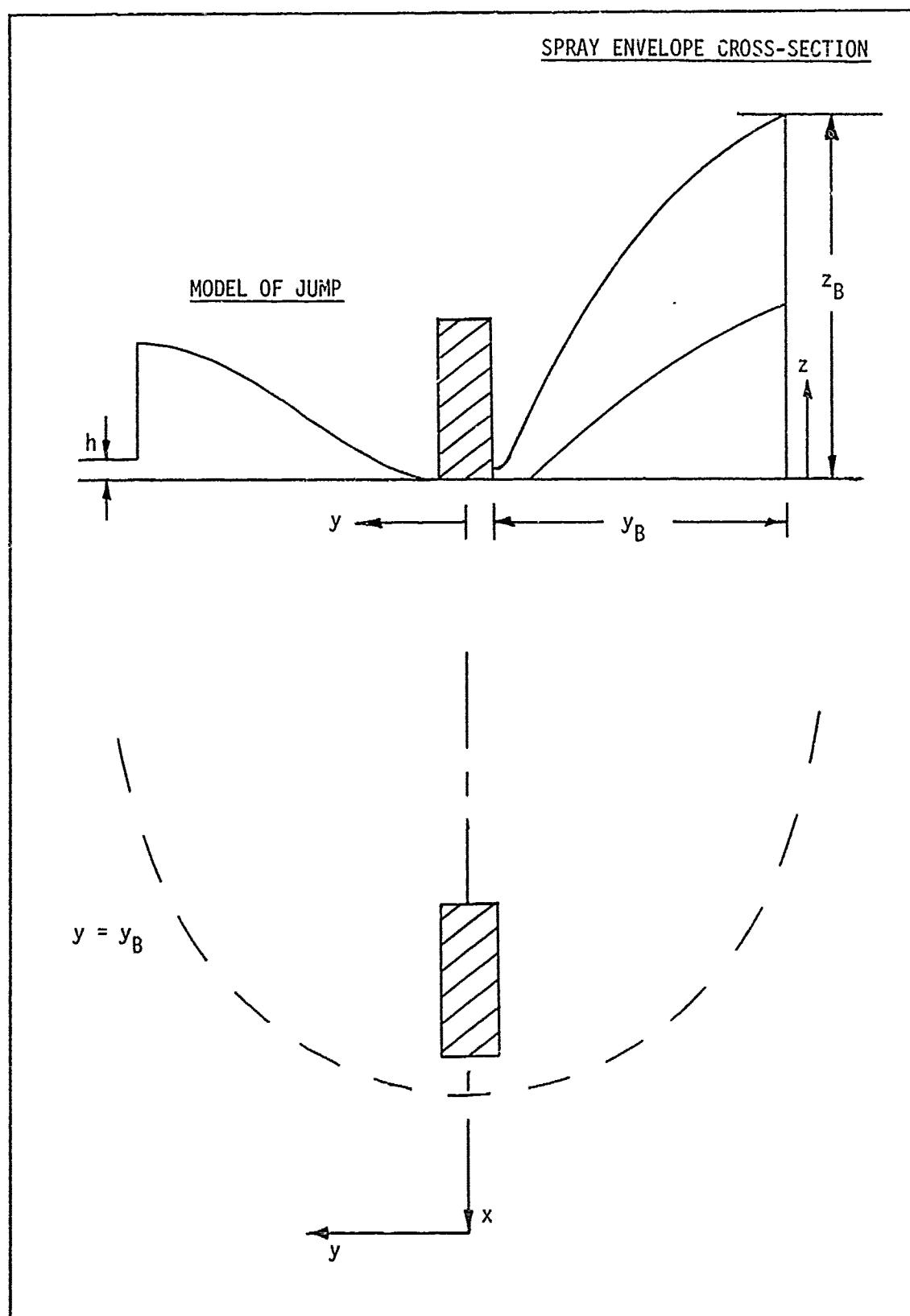
74

FIGURE A.I.1
DYNAMICS OF WHEEL SPRAY

75

APPENDIX II

Flow Equations

All symbols used are defined under Nomenclature.

II.1. Three-dimensional Flow Equations in Intrinsic Coordinates

a) Mass Conservation Equations:

Gas Phase

$$\frac{1}{r}\left[\frac{\delta}{\partial m}\left(r\,[1-\sigma_v]\,\rho_g\,W_{gm}\right) + \frac{\delta}{\partial \vartheta}\left([1-\sigma_v]\,\rho_g\,W_{g\vartheta}\right) + \frac{\delta}{\partial n}\left(r\,[1-\sigma_v]\,\rho_g\,W_{gn}\right)\right.$$

$$+\frac{\delta}{\partial m}\left(r\,[1-\sigma_v]\,\rho_g\,U_m\right) + \frac{\delta}{\partial \vartheta}\left([1-\sigma_v]\,\rho_g\,U_\vartheta\right) \tag{A.II.1}$$

$$\left.+\frac{\delta}{\partial n}\left(r\,[1-\sigma_v]\,\rho_g\,U_n\right)\right] = \dot{m}_v$$

Liquid Phase

$$\frac{1}{r}\left[\frac{\delta}{\partial m}\left(r\,\sigma_v\,\rho_p\,W_{pm}\right) + \frac{\delta}{\partial \vartheta}\left(\sigma_v\,\rho_p\,W_{p\vartheta}\right) + \frac{\delta}{\partial n}\left(r\,\sigma_v\,\rho_p\,W'_{pn}\right)\right.$$

$$+\frac{\delta}{\partial m}\left(r\,\sigma_v\,\rho_p\,U_m\right) + \frac{\delta}{\partial \vartheta}\left(\sigma_v\,\rho_p\,U_\vartheta\right) \tag{A.II.2}$$

$$\left.+\frac{\delta}{\partial n}\left(r\,\sigma_v\,\rho_p\,U_n\right)\right] = -\dot{m}_v$$

76

b) Momentum Conservation Equations:

Gas Phase

m-component

$$(1-\sigma_v)\rho_g\left[(W_{gm}+U_m)\left(\frac{\delta W_{gm}}{\delta m}+\frac{\delta U_m}{\delta m}\right)-\frac{(W_{g\theta}+U_\theta)}{r}\times\right.$$

$$\left.\left((W_{g\theta}+U_\theta)\frac{\delta r}{\delta m}-\frac{\delta W_{gm}}{\delta\theta}-\frac{\delta U_m}{\delta\theta}\right)\right]$$

$$=-\frac{\delta P_g}{\delta m}+F_{Bgm}+F_{Vgm}+F_{Im} \qquad\qquad (A.II.3)$$

θ-component

$$(1-\sigma_v)\rho_g\left[\frac{(W_{gm}+U_m)}{r}\left(\frac{\delta r W_{g\theta}}{\delta m}+\frac{\delta r U_\theta}{\delta m}\right)\right.$$

$$\left.+\frac{(W_{g\theta}+U_\theta)}{r}\left(\frac{\delta W_{g\theta}}{\delta\theta}+\frac{\delta U_\theta}{\delta\theta}\right)\right]=-\frac{1}{r}\frac{\delta P_g}{\delta\theta} \qquad (A.II.4)$$

$$+F_{Bg\theta}+F_{Vg\theta}+F_{I\theta}$$

n-component

$$(1 - \sigma_v) \rho_g \left[\left(W_{gm} + U_m \right) \left(\delta \frac{W_{gn}}{\partial m} + \frac{\delta U_n}{\partial m} \right) - \frac{\left(W_{g\theta} + U_\theta \right)}{r} \right.$$

$$\left. \left(\left(W_{g\theta} + U_\theta \right) \frac{\delta r}{\partial n} - \frac{\delta W_{gn}}{\partial \theta} - \frac{\delta U_n}{\partial \theta} \right) \right] \qquad (A.II.5)$$

$$= - \frac{\delta P_g}{\partial n} + F_{B_{gn}} + F_{V_{gn}} + F_{I_n}$$

Liquid Phase

m-component

$$\sigma_v \rho_P \left[\left(W_{Pm} + U_m \right) \left(\frac{\delta W_{Pm}}{\partial m} + \frac{\delta U_m}{\partial m} \right) - \frac{\left(W_{P\theta} + U_\theta \right)}{r} \times \right.$$

$$\left. \left(\left(W_{P\theta} + U_\theta \right) \frac{\delta r}{\partial m} - \frac{\delta W_{Pm}}{\partial \theta} - \frac{\delta U_m}{\partial \theta} \right) \right] \qquad (A.II.6)$$

$$= F_{B_{Pm}} + F_{V_{Pm}} - F_{I_m}$$

θ-component

$$\sigma_v \rho_p \left[\frac{(W_{pm} + U_m)}{r} \left(\frac{\delta r \, W_{p\theta}}{\partial m} + \frac{\delta r \, U_\theta}{\partial m} \right) + \frac{(W_{p\theta} + U_\theta)}{r} \times \right.$$

$$\left. \left(\frac{\delta W_{p\theta}}{\partial \theta} + \frac{\delta U_\theta}{\partial \theta} \right) \right] = F_{B_{p\theta}} + F_{V_{p\theta}} - F_{I\theta} \qquad \text{(A.II.7)}$$

n-component

$$\sigma_v \rho_p \left[(W_{pm} + U_m) \left(\frac{\delta W_{pn}}{\partial m} + \frac{\delta U_n}{\partial m} \right) - \frac{(W_{p\theta} + U_\theta)}{r} \times \right.$$

$$\left. \left((W_{p\theta} + U_\theta) \frac{\delta r}{\partial n} - \frac{\delta W_{pn}}{\partial \theta} - \frac{\delta U_n}{\partial \theta} \right) \right] = F_{B_{p_n}} + F_{V_{pn}} - F_{I_n} \qquad \text{(A.II.8)}$$

c) Energy Conservation Equations:

Gas Phase

$$(1 - \sigma_v) \rho_g \left[(W_{gm} + U_m) \frac{\delta h_g}{\partial m} + \frac{(W'_{g\theta} + U'_\theta)}{r} \frac{\delta h_g}{\partial \theta} \right]$$

$$= \Phi_g + \Phi_I + \bar{P}_g + (W_{gm} + U_m) \frac{\delta P_g}{\partial m} + \frac{(W_{g\theta} + U_\theta)}{r} \frac{\delta P_g}{\partial \theta} \qquad \text{(A.II.9)}$$

$$- \frac{\delta q'_{gm}}{\partial m} - \frac{\delta q'_{Im}}{\partial m} - \frac{1}{r} \left[\frac{\delta q'_{g\theta}}{\partial \theta} + \frac{\delta q'_{I\theta}}{\partial \theta} \right] - \frac{\delta q'_{gn}}{\partial n} - \frac{\delta q'_{In}}{\partial n}$$

79

Liquid Phase

$$\sigma_v \rho_p \left[(W_{pm} + U_m) \frac{\delta u_p}{\delta m} + \frac{(W_{p\theta} + U_\theta)}{r} \frac{\delta u_p'}{\delta \theta} \right] = \mathcal{F}_p - \mathcal{F}_1 + \bar{P}_p$$

(A.II.10)

$$- \frac{\delta q'_{p_m}}{\delta m} + \frac{\delta q'_{I_m}}{\delta m} - \frac{1}{r} \left(\frac{\delta q'_{p\theta}}{\delta \theta} - \frac{\delta q'_{I\theta}}{\delta \theta} \right) - \frac{\delta q'_{p_n}}{\delta n} + \frac{\delta q'_{I_n}}{\delta n}$$

d) Variation of σ_v with respect to the three coordinate directions:

m-direction

The equation is obtained as follows. The θ-component gas phase momentum conservation equation is differentiated with respect to θ. Next the m-component gas phase momentum conservation equation is solved in terms of ($1 - \sigma_v$). These two equations are then combined with the gas phase mass conservation equation to obtain the final result.

$$\frac{\delta \sigma_v}{\delta m} = - \frac{\dot{m}_v}{\rho_g (W_{gm} + U_m)} + \frac{(W_{g\theta} + U_\theta)}{r \rho_g (W_{gm} + U_m)} \frac{\delta}{\delta \theta} \left(F_{Bg\theta} + F_{Vg\theta} + F_{I\theta} - \frac{1}{r} \frac{\delta P_g}{\delta \theta} \right)$$

$$\left[\frac{(W_{gm} + U_m)}{r} \left(\frac{\delta r W_{g\theta}}{\delta m} + \frac{\delta r U_\theta}{\delta m} \right) + \frac{(W_{g\theta} + U_\theta)}{r} \left(\frac{\delta W_{g\theta}}{\delta \theta} + \frac{\delta U_\theta}{\delta \theta} \right) \right]^{-1}$$

$$+ \frac{1}{r \rho_g^2 (W_{gm} + U_m)} \left[F_{Bgm} + F_{Vgm} + F_{Im} - \frac{\delta P_g}{\delta m} \right] \left[(W_{gm} + U_m) \left(\frac{\delta W_{gm}}{\delta m} + \frac{\delta U_m}{\delta m} \right) \right.$$

$$\left. - \frac{(W_{g\theta} + U_\theta)}{r} \left((W_{g\theta} + U_\theta) \frac{\delta r}{\delta m} - \frac{\delta W_{gm}}{\delta \theta} - \frac{\delta U_m}{\delta \theta} \right) \right]^{-1} \times$$

80

$$\left\{ \frac{\delta}{\delta m}\left(r\rho_g W_{gm}\right) + \frac{\delta}{\delta m}\left(r\rho_g U_m\right) + \rho_g\frac{\delta W_{g\theta}}{\delta\theta} + \rho_g\frac{\delta U_\theta}{\delta\theta} + \frac{\delta}{\delta n}\left(r\rho_g W_{gn}\right) + \frac{\delta}{\delta n}\left(r\rho_g U_n\right) \right.$$

$$-\left(W_{g\theta}+U_\theta\right)\rho_g\frac{\delta}{\delta\theta}\left[\frac{\left(W_{gm}+U_m\right)}{r}\left(\frac{\delta r W_{g\theta}}{\delta m} + \frac{\delta r U_\theta}{\delta m}\right)+\frac{\left(W_{g\theta}+U_\theta\right)}{r}\left(\frac{\delta W_{g\theta}}{\delta\theta} + \frac{\delta U_\theta}{\delta\theta}\right)\right]$$

$$\left. \left[\frac{\left(W_{gm}+U_m\right)}{r}\left(\frac{\delta r W_{g\theta}}{\delta m} + \frac{\delta r U_\theta}{\delta m}\right) + \frac{\left(W_{g\theta}+U_\theta\right)}{r}\left(\frac{\delta W_{g\theta}}{\delta\theta} + \frac{\delta U_\theta}{\delta\theta}\right)\right]^{-1} \right\}$$

(A.II.11)

θ-direction

The m-component gas phase momentum conservation equation is differentiated with respect to m. Next the θ-component gas phase momentum conservation equation is solved in terms of ($1 - \sigma_v$). These two equations are then combined with the gas phase mass conservation equation to obtain the final result.

$$\frac{\delta\sigma_v}{\delta\theta} = \frac{-r\dot{m}_v}{\rho_g\left(W_{g\theta}+U_\theta\right)} + \frac{r\left(W_{gm}+U_m\right)}{\rho_g\left(W_{g\theta}+U_\theta\right)}\frac{\delta}{\delta m}\left(F_{\theta_{g_m}} + F_{V_{g_m}} + F_{I_m} - \frac{\delta P_g}{\delta m}\right)\times$$

$$\left[\frac{\delta}{\delta m}\left(r\rho_g W_{gm}\right) + \frac{\delta}{\delta m}\left(r\rho_g U_m\right) + \frac{\delta}{\delta\theta}\left(\rho_g W_{g\theta}\right) + \frac{\delta}{\delta\theta}\left(\rho_g U_\theta\right) + \frac{\delta}{\delta n}\left(r\rho_g W_{gn}\right) + \frac{\delta}{\delta n}\left(r\rho_g U_n\right)\right]^{-1}$$

$$+\frac{1}{\rho_g^2\left(W_{g\theta}+U_\theta\right)}\left[F_{\theta_{g\theta}} + F_{V_{g\theta}} + F_{I\theta} - \frac{1}{r}\frac{\delta P_g}{\delta\theta}\right]\left[\frac{\left(W_{gm}+U_m\right)}{r}\left(\frac{\delta r W_{g\theta}}{\delta m} + \frac{\delta r U_\theta}{\delta m}\right)\right.$$

81

$$+ \frac{(W_{g\theta} + U_\theta)}{r} \left(\frac{\delta W_{g\theta}}{\partial \theta} + \frac{\delta U_\theta}{\partial \theta} \right) \Bigg]^{-1} \left\{ \rho_g \frac{\delta (r W_{gm})}{\partial n} + \rho_g \frac{\delta}{\partial m} (r U_m) + \frac{\delta}{\partial \theta} (\rho_g W_{g\theta}) \right.$$

$$+ \frac{\delta}{\partial \theta} (\rho_g U_\theta) + \frac{\delta}{\partial n} (r \rho_g W_{gn}) + \frac{\delta}{\partial n} (r \rho_g U_n) - r \rho_g (W_{gm} + U_m) \times \quad \text{(A.II.12)}$$

$$\frac{\delta}{\partial m} \left[\frac{\delta}{\partial m}(r\rho_g W_{gm}) + \frac{\delta}{\partial m}(r\rho_g U_m) + \frac{\delta}{\partial \theta}(\rho_g W_{g\theta}) + \frac{\delta}{\partial \theta}(\rho_g U_\theta) + \frac{\delta}{\partial n}(r\rho_g W_{gn}) + \frac{\delta}{\partial n}(r\rho_g U_n) \right]$$

$$\times \left[\frac{\delta}{\partial m}(r\rho_g W_{gm}) + \frac{\delta}{\partial m}(r\rho_g U_m) + \frac{\delta}{\partial \theta}(\rho_g W_{g\theta}) + \frac{\delta}{\partial \theta}(\rho_g U_\theta) + \frac{\delta}{\partial n}(r\rho_g W_{gn}) + \frac{\delta}{\partial n}(r\rho_g U_n) \right]^{-1} \Bigg\}$$

n-direction

The equation is obtained by first differentiating the n-component gas phase momentum conservation equation with respect to n. Then the θ-component gas phase momentum conservation equation is solved in terms of ($1 - \sigma_v$) and combined with the differentiated n-component gas phase momentum conservation equation to obtain the final result.

$$\frac{\delta \sigma_v}{\partial n} = -\frac{\delta}{\partial n} \left[F_{B_j} + F_{V_{gn}} + F_{I_n} - \frac{\delta P_g}{\partial n} \right] \frac{1}{\rho_g} \left[(W_{gm} + U_m) \left(\frac{\delta W_{gn}}{\partial m} + \frac{\delta U_n}{\partial m} \right) \right.$$

$$\left. - \frac{(W_{g\theta} + U_\theta)}{r} \left((W_{g\theta} + U_\theta) \frac{\delta r}{\partial n} - \frac{\delta W_{gn}}{\partial \theta} - \frac{\delta U_n}{\partial \theta} \right) \right]^{-1}$$

$$+ \left[F_{B_{g\theta}} + F_{V_{g\theta}} + F_{I\theta} - \frac{1}{r} \frac{\delta P_g}{\partial \theta} \right] \frac{1}{\rho_g} \left[\frac{(W_{gm} + U_m)}{r} \left(\frac{\delta}{\partial m}(r W_{g\theta}) + \frac{\delta}{\partial m}(r U_\theta) \right) \right.$$

$$+ \left(\frac{W_{g\theta} + U_\theta}{r}\right)\left(\frac{\delta W_{g\theta}}{\delta \theta} + \frac{\delta U_\theta}{\delta \theta}\right)\Bigg]^{-1}\left\{\frac{1}{\rho_g}\frac{\delta \rho_g}{\delta n} + \frac{\delta}{\delta n}\Bigg[(W_{gm} + U_m) \times\right.$$

$$\left(\frac{\delta W_{gn}}{\delta m} + \frac{\delta U_n}{\delta m}\right) - \left(\frac{W_{g\theta} + U_\theta}{r}\right)\left((W_{g\theta} + U_\theta)\frac{\delta r}{\delta n} - \frac{\delta W_{gr}}{\delta \theta} - \frac{\delta U_n}{\delta \theta}\right)\Bigg] \times$$

$$\Bigg[(W_{gm} + U_m)\left(\frac{\delta W_{gn}}{\delta m} + \frac{\delta U_n}{\delta m}\right) - \left(\frac{W_{g\theta} + U_\theta}{r}\right) \times$$

$$\left((W_{g\theta} + U_\theta)\frac{\delta r}{\delta n} - \frac{\delta W_{gn}}{\delta \theta} - \frac{\delta U_n}{\delta \theta}\right)\Bigg]^{-1}\Bigg\}$$

(A.II.13)

e) Equilibrium Equations:

Gas Phase

An enthalpy-entropy relation valid for the gas-phase flow can be written as follows.

$$\frac{d\rho_g}{(1-\sigma_v)\rho_g} = dh_g + \frac{1}{(1-\sigma_v)\rho_g}\Big[-T_g\,ds_g - T_{gp}\,ds_I + dq_g + dq_I\Big]$$

(A.II.14)

where

h_g = enthalpy of the gas phase per unit mass of the gas phase (joules/Kg$_g$)

ds_g = rise in entropy of the gas phase (per unit volume of mixture) due to the action of body and surface forces on the gas phase, excluding those forces imposed by the liquid phase (joules/°K Vol$_m$)

83

T_{jp} = mass averaged gas phase-liquid phase temperature (°K)

ds_1 = rise in entropy of the gas phase (per unit volume of mixture)
due to the action of forces on the gas phase imposed by the
liquid phase (joules/°K Vol$_{\overline{m}}$)

dq_{3} = the heat loss from the gas phase (per unit volume of mixture)
to the surroundings, excluding the heat lost directly to the
liquid phase (joules/Vol$_{\overline{m}}$)

dq_{I} = heat loss from the gas phase (per unit volume of mixture)
directly to the liquid phase (joules/Vol$_{\overline{m}}$).

By definition

$$H_{3} = h_{3} + V_{3}^{2}/2 \qquad\qquad\text{(A.II.15)}$$

where

H_{3} = total enthalpy of the gas phase per unit mass of the gas phase
(joules/Kg$_g$).

Combining (A.II.14) and (A.II.15),

$$\frac{dp_{3}}{(1-\sigma_{v})\rho_{3}} = dH_{3} - V_{3m}\,dV_{3m} - V_{30}\,dV_{30} + \frac{1}{(1-\sigma_{v})\rho_{3}} \times$$
$$\left[-T_{3}\,ds_{3} - T_{3p}\,ds_{I} + dq_{3} + dq_{I} \right]. \qquad\text{(A.II.16)}$$

Combining (A.II.16) with each of the component gas phase momentum
equations (eliminating the pressure gradient term) yields the following
equilibrium results.

m-component

$$(1 - \sigma_{v})\rho_{3}\,\frac{(W_{30} + U_{\theta})}{r}\left[\frac{\delta W_{3m}}{\partial\theta} + \frac{\delta U_{m}}{\partial\theta} - \frac{\delta\,r\,W_{30}}{\partial m} - \frac{\delta\,r\,U_{\theta}}{\partial m}\right]$$

84

$$= F_{B_{gm}} + F_{V_{gm}} + F_{Im} - \rho_g [1 - \sigma_r] \frac{\delta H_g}{\partial m} + T_g \frac{\delta s_g}{\partial m}$$

$$+ T_{gp} \frac{\delta s_I}{\partial m} - \frac{\delta q_g}{\partial m} - \frac{\delta q_I}{\partial m} \qquad \text{(A.II.17)}$$

θ-component

$$(1 - \sigma_r) \rho_g \frac{(W_{gm} + U_m)}{r} \left[\frac{\delta}{\partial m}(r W_{g\theta}) + \frac{\delta}{\partial m}(r U_\theta) - \frac{\delta W_{gm}}{\partial \theta} \right.$$

$$\left. - \frac{\delta U_m}{\partial \theta} \right] = F_{B_{g\theta}} + F_{V_{g\theta}} + F_{I\theta} + \frac{1}{r} \left[-(1 - \sigma_r) \rho_g \frac{\delta H_g}{\partial \theta} \right. \qquad \text{(A.II.18)}$$

$$\left. + T_g \frac{\delta s_g}{\partial \theta} + T_{gp} \frac{\delta s_I}{\partial \theta} - \frac{\delta q_g}{\partial \theta} - \frac{\delta q_I}{\partial \theta} \right]$$

n-component

$$(1 - \sigma_r) \rho_g \left[(W_{gm} + U_m) \left(\frac{\delta W_{gn}}{\partial m} + \frac{\delta U_n}{\partial m} - \frac{\delta W_{gm}}{\partial n} - \frac{\delta U_m}{\partial n} \right) \right.$$

$$\left. - \frac{(W_{g\theta} + U_\theta)}{r} \left(\frac{\delta r W_{g\theta}}{\partial n} + \frac{\delta r U_\theta}{\partial n} - \frac{\delta W_{gn}}{\partial \theta} - \frac{\delta U_n}{\partial \theta} \right) \right]$$

85

$$= F_{Bg_n} + F_{Vg_n} + F_{I_n} - \rho_g \left[1 - \sigma_v \right] \frac{\delta H_g}{\partial n} + T_g \frac{\delta s_g}{\partial n}$$

$$+ T_{gp} \frac{\delta s_I}{\partial n} - \frac{\delta q_g}{\partial n} - \frac{\delta q_I}{\partial n} \qquad \text{(A.II.19)}$$

Liquid Phase

An internal energy-entropy relation valid for the liquid phase flow can be written as follows.

$$d u_p = \frac{1}{\sigma_v \rho_p} \left[T_p \, d s_p - T_{gp} \, d s_I - d q_p + d q_I \right] \qquad \text{(A.II.20)}$$

where

u_p = internal energy of the liquid phase per unit mass of the liquid phase (joules/Kg_p)

$d s_p$ = rise in entropy of the liquid phase (per unit volume of mixture) due to the action of body and surface forces on the liquid phase, excluding those forces imposed by the gas phase (joules/°K $Vol_{\overline{m}}$)

$d q_p$ = heat loss from the liquid phase (per unit volume of mixture) to the surroundings, excluding the heat lost directly to the gas phase (joules/$Vol_{\overline{m}}$).

86

By definition

$$U_p = u_p + V_p^2/2 \tag{A.II.21}$$

where

U_p = total internal energy of the liquid phase per unit mass of the liquid phase (joules/Kg_p).

Combining (A.II.20) with (A.II.21) and expanding

$$d U_p = V_{pm}\, d V_{pm} + V_{p\theta}\, d V_{p\theta} + \frac{1}{\sigma_v \rho_p} \times$$

$$\left[T_p\, d s_p - T_{\mathfrak{I} p}\, d s_{\mathfrak{I}} - d q_p + d q_{\mathfrak{I}} \right]. \tag{A.II.22}$$

Combining (A.II.22) with each of the component liquid phase momentum conservation equations yields the following equilibrium results.

u-underline **m-component**

$$\sigma_v \rho_p \frac{(W_{p\theta}+U_\theta)}{r} \left[\frac{\delta W_{pm}}{\partial \theta} + \frac{\delta U_m}{\partial \theta} - \frac{\delta(r W_{p\theta})}{\partial m} - \frac{\delta(r U_\theta)}{\partial m} \right]$$

$$= F_{B p m} + F_{V p m} - F_{\mathfrak{I} m} - \sigma_v \rho_p \frac{\delta U_p}{\partial m} + T_p \frac{\delta s_p}{\partial m} - T_{\mathfrak{I} p} \frac{\delta s_{\mathfrak{I}}}{\partial \theta} \tag{A.II.23}$$

$$- \frac{\delta q_p}{\partial m} + \frac{\delta q_{\mathfrak{I}}}{\partial m}$$

θ-component

$$\sigma_v \rho_p \frac{(W_{pm}+U_m)}{r} \left[\frac{\delta(r W_{p\theta})}{\partial m} + \frac{\delta(r U_\theta)}{\partial m} - \frac{\delta W_{pm}}{\partial \theta} - \frac{\delta U_m}{\partial \theta} \right]$$

$$= F_{B p \theta} + F_{V p \theta} - F_{\mathfrak{I} \theta} + \frac{1}{r} \left[-\sigma_v \rho_p \frac{\delta U_p}{\partial \theta} + T_p \frac{\delta s_p}{\partial \theta} - T_{\mathfrak{I} p} \frac{\delta s_{\mathfrak{I}}}{\partial \theta} \right. \tag{A.II.24}$$

$$\left. - \frac{\delta q_p}{\partial \theta} + \frac{\delta q_{\mathfrak{I}}}{\partial \theta} \right] \qquad 87$$

<u>n-component</u>

$$\sigma_v \rho_p \left[\left(W_{prn} + U_m \right) \left(\frac{\delta W_{pn}}{\delta m} + \frac{\delta U_n}{\delta m} - \frac{\delta W_{pm}}{\delta n} - \frac{\delta U_m}{\delta n} \right) \right.$$

$$\left. - \frac{\left(W_{p\theta} + U_\theta \right)}{r} \left(\frac{\delta (r W_{p\theta})}{\delta n} + \frac{\delta (r U_\theta)}{\delta n} - \frac{\delta W_{pn}}{\delta \theta} - \frac{\delta U_n}{\delta \theta} \right) \right] \tag{A.II.25}$$

$$= F_{B_{pn}} + F_{V_{pn}} - F_{I_n} - \sigma_v \rho_p \frac{\delta U_p}{\delta n} + T_p \frac{\delta s_p}{\delta n} - T_{gp} \frac{\delta s_I}{\delta n}$$

$$- \frac{\delta J_p}{\delta n} + \frac{\delta g_I}{\delta n}$$

II.2. <u>Axisymmetric Flow Equations in Intrinsic Coordinates</u>

  a) Mass Conservation Equations:

<u>Gas Phase</u>

$$\frac{1}{r} \left[\frac{\delta}{\delta m} \left(r \left[1 - \sigma_v \right] \rho_g W_{gm} \right) + r \left(1 - \sigma_v \right) \rho_g \frac{\delta W_{gn}}{\delta n} \right] = \dot{m}_v \tag{A.II.26}$$

<u>Liquid Phase</u>

$$\frac{1}{r} \left[\frac{\delta}{\delta m} \left(r \sigma_v \rho_p W_{pm} \right) + r \sigma_v \rho_p \frac{\delta W_{pn}}{\delta n} \right] = - \dot{m}_v \tag{A.II.27}$$

88

b) Momentum Conservation Equations:

Gas Phase

m-component

$$(1-\sigma_v)\rho_g\left[W_{gm}\frac{\delta W_{gm}}{\partial m}-\frac{(W_{g\theta}+r\omega)^2}{r}\frac{\delta r}{\partial m}\right]$$

$$= -\frac{\delta P_g}{\partial m} + F_{B_{gm}} + F_{V_{gm}} + F_{I_m} \tag{A.II.28}$$

θ-component

$$(1-\sigma_v)\rho_g\frac{W_{gm}}{r}\left(\frac{\delta(r\,W_{g\theta})}{\partial m}+2\omega r\frac{\delta r}{\partial m}\right)$$

$$= F_{B_{g\theta}} + F_{V_{g\theta}} + F_{I\theta} \tag{A.II.29}$$

n-component

$$(1-\sigma_v)\rho_g\left[W_{gm}\frac{\delta W_{gn}}{\partial m}-\frac{(W_{g\theta}+r\omega)^2}{r}\frac{\delta r}{\partial n}\right]$$

$$= -\frac{\delta P_g}{\partial n} + F_{B_{gn}} + F_{V_{gn}} + F_{I_n} \tag{A.II.30}$$

Liquid Phase

m-component

$$\sigma_v\rho_p\left[W_{pm}\frac{\delta W_{pm}}{\partial m}-\frac{(W_{p\theta}+r\omega)^2}{r}\frac{\delta r}{\partial m}\right]$$

$$= F_{B_{pm}} + F_{V_{pm}} - F_{I_m} \tag{A.II.31}$$

89

θ-component

$$\sigma_\gamma \rho_P \frac{W_{\rho m}}{r} \left(\frac{\delta (r \, W_{\rho \theta})}{\partial m} + 2 \, \omega \, r \, \frac{\delta r}{\partial m} \right)$$

(A.II.32)

$$= F_{B_{P\theta}} + F_{V_{P\theta}} - F_{I\theta}$$

n-component

$$\sigma_\gamma \rho_P \left[W_{\rho m} \frac{\delta W_{\rho n}}{\partial m} - \frac{(W_{\rho \theta} + r \omega)^2}{r} \frac{\delta r}{\partial n} \right]$$

(A.II.33)

$$= F_{B_{\rho n}} + F_{V_{\rho n}} - F_{In}$$

c) Energy Conservation Equations:

Gas Phase

$$(1 - \sigma_\gamma) \rho_g \, W_{gm} \frac{\delta h_{ig}}{\partial m} = \mathcal{I}_g + \Phi_I + \bar{P}_g + W_{gm} \frac{\delta P_g}{\partial m}$$

(A.II.34)

$$- \frac{\delta q'_{gm}}{\partial m} - \frac{\delta q'_{Im}}{\partial m} - \frac{\delta q'_{gn}}{\partial n} - \frac{\delta q'_{In}}{\partial n}$$

Liquid Phase

$$\sigma_\gamma \rho_P \, W_{Fm} \frac{\delta u_\rho}{\partial m} = \mathcal{I}_P - \mathcal{I}_I + \bar{P}_P - \frac{\delta q'_{Pm}}{\partial m}$$

(A.II.35)

$$+ \frac{\delta q'_{Im}}{\partial m} - \frac{\delta q'_{Pn}}{\partial n} + \frac{\delta q'_{In}}{\partial n}$$

90

d) Variation of σ_v with respect to the three coordinate directions:

<u>m-direction</u>

$$\frac{\delta \sigma_v}{\partial m} = -\frac{\dot{m}_v}{\rho_j W_{jm}} + \left[F_{B_{jm}} + F_{V_{jm}} + F_{J_m} - \frac{\delta P_j}{\partial m} \right] \frac{1}{r \rho_j^2 W'_{jm}} \quad ,$$

$$\left[W_{jm} \frac{\delta W_{jm}}{\partial m} - \frac{(W_{j\theta} + r\omega)^2}{r} \frac{\delta r}{\partial m} \right]^{-1} \times \qquad\qquad \text{(A.II.36)}$$

$$\left[\frac{\delta}{\partial m} (r \rho_j W_{jm}) + \frac{\delta}{\partial n} (r \rho_j W_{jn}) \right]$$

<u>θ-direction</u>

$$\frac{\delta \sigma_v}{\partial \theta} = 0 \qquad\qquad\qquad\qquad \text{(A.II.37)}$$

<u>n-direction</u>

$$\frac{\delta \sigma_v}{\partial n} = -\frac{\delta}{\partial n} \left[F_{B_{jn}} + F_{V_{jn}} + F_{I_n} - \frac{\delta P_j}{\partial n} \right] \frac{1}{\rho_j} \left[W_{jm} \frac{\delta W_{jn}}{\partial m} \right.$$

$$\left. -\frac{(W'_{j\theta} + r\omega)^2}{r} \frac{\delta r}{\partial n} \right]^{-1} + \left[F_{B_{j\theta}} + F_{V_{j\theta}} + F_{I\theta} \right] \left[\rho_j \frac{W_{jm}}{r} \right. \times$$

$$\left(\frac{\delta}{\partial m} (r W_{j\theta}) + 2\omega r \frac{\delta r}{\partial m} \right) \right]^{-1} \times \left\{ \frac{1}{\rho_j} \frac{\delta \rho_j}{\partial n} \right.$$

$$+ \frac{S}{\partial n} \left[W_{gm} \frac{\delta W_{gr}}{\partial m} - \frac{(W_{go} + r\omega)^2}{r} \frac{\delta r}{\partial n} \right] \cdot$$

$$\left[W_{gm} \frac{\delta W_{gn}}{\partial m} - \frac{(W_{go} + r\omega)^2}{r} \frac{\delta r}{\partial n} \right]^{-1} \Bigg\}$$

(A.II.38)

e) Radial Equilibrium Equation:

These equations are deduced utilizing the method of Wennerstrom (Ref. 56).

<u>Gas Phase</u>

$$W_{gm} \frac{dW_{gm}}{dL} = \sin(\phi - \gamma_c) W_{gm} \frac{\delta W_{gm}}{\partial r} + \cos(\phi - \gamma_c) \frac{W_{gm}^2}{r_c} - \frac{W_{go}}{r} \frac{d}{dL}(r W_{go})$$

$$- 2\omega W_{go} \cos \gamma_c + \frac{d I_g}{dL} + \left[-T_g \frac{ds_g}{dL} - T_{gp} \frac{ds_I}{dL} + \frac{dq_g}{dL} \right.$$

(A.II.39)

$$\left. + \frac{dq_I}{dL} \right] \frac{1}{(1 - \sigma_v) \rho_g} - \left[F_{Bgm} + F_{vgm} + F_{Im} \right] \frac{\sin(\phi - \gamma_c)}{(1 - \sigma_v) \rho_g}$$

$$- \left[\Gamma_{Bgn} + \Gamma_{vgn} + \Gamma_{In} \right] \frac{\cos(\phi - \gamma_c)}{(1 - \sigma_v) \rho_g}$$

92

Liquid Phase

$$W_{pm} \frac{d W_{pm}}{dL} = \sin(\phi - r_c) \, W_{pm} \frac{\delta W_{pm}}{\delta m} + \cos(\phi - r_c) \frac{W_{pm}^2}{r_c}$$

$$- \left(\frac{W_{p\theta}}{r} + \omega \right) \left(\frac{d}{dL}(r\, W_{q\theta}) + 2\, r \omega \cos r_c \right) + \frac{d\, U_p}{dL}$$

$$- \frac{\sin(\phi - r_c)}{\sigma_r \rho_p} \left[F_{\beta_{pm}} + F_{V_{pm}} - F_{I_m} \right] \hspace{2cm} \text{(A.II.40)}$$

$$- \frac{\cos(\phi - r_c)}{\sigma_r \rho_p} \left[F_{\beta_{pn}} + F_{V_{pn}} - F_{I_n} \right] + \frac{1}{\sigma_r \rho_p} \left[-T_p \frac{ds_p}{dL} + T_{qp} \frac{ds_I}{dL} + \frac{d\, q_p}{dL} - \frac{d\, q_I}{dL} \right]$$

It may be pointed out here that in general three-dimensional flow, it is necessary to set up equilibrium conditions in all of the three directions (Eqs. A.II.17, A.II.18, A.II.19 and A.II.23, A.II.25, A.II.25).

II.3. Three-dimensional Flow Equations in Cylindrical Coordinates

a) Mass Conservation Equations:

Gas Phase

$$\frac{1}{r} \frac{\delta}{dr} \left(r[1 - \sigma_r] \rho_g W_{gr} \right) + \frac{1}{r} \frac{\delta}{d\theta} \left([1 - \sigma_r] \rho_g W_{g\theta} \right)$$

$$+ \frac{\delta}{dz} \left([1 - \sigma_r] \rho_g W_{gz} \right) + \omega \frac{\delta}{d\theta} \left([1 - \sigma_r] \rho_g \right) = \dot{m}_v \hspace{1.5cm} \text{(A.II.41)}$$

93

Liquid Phase

$$\frac{1}{r} \frac{\delta}{\delta r} \left(\sigma_v \rho_p \, r \, W_{pr} \right) + \frac{1}{r} \frac{\delta}{\delta \theta} \left(\sigma_v \rho_p \, W_{p\theta} \right)$$

$$\frac{\delta}{\delta z} \left(\sigma_v \rho_p \, W_{pz} \right) + \omega \frac{\delta}{\delta \theta} \left(\sigma_v \rho_p \right) = - \dot{m}_v \qquad \text{(A.II.42)}$$

b) Momentum Conservation Equations:

Gas Phase

r-component

$$(1-\sigma_v) \rho_g \left[W_{gr} \frac{\delta W_{gr}}{\delta r} + \left(\frac{W_{g\theta}}{r} + \omega \right) \frac{\delta W_{gr}}{\delta \theta} \right.$$

$$\left. - \frac{(W_{g\theta} + r\omega)^2}{r} + W_{gz} \frac{\delta W_{gr}}{\delta z} \right] = - \frac{\delta P_g}{\delta r} \qquad \text{(A.II.43)}$$

$$+ F_{Bgr} + F_{V_{gr}} + F_{Ir}$$

θ-component

$$(1-\sigma_v) \rho_g \left[W_{gr} \left(\frac{\delta W_{g\theta}}{\delta r} + \omega \right) + \left(\frac{W_{g\theta}}{r} + \omega \right) \frac{\delta W_{g\theta}}{\delta \theta} \right.$$

$$\qquad \text{(A.II.44)}$$

$$\left. + W_{gr} \left(\frac{W_{g\theta}}{r} + \omega \right) + W_{gz} \frac{\delta W_{g\theta}}{\delta z} \right] = -\frac{1}{r} \frac{\delta P_g}{\delta \theta} + F_{Bg\theta} + F_{V_{g\theta}} + F_{I\theta}$$

94

z-component

$$(1-\sigma_r)\rho_g \left[W_{gr} \frac{\delta W_{gz}}{\partial r} + \left(\frac{W_{g\theta}}{r} + \omega \right) \frac{\delta W_{gz}}{\partial \theta} + W_{gz} \frac{\delta W_{gz}}{\partial z} \right]$$

$$= -\frac{\delta P_g}{\partial z} + F_{Bgz} + F_{Vgz} + F_{Iz} \qquad \text{(A.II.45)}$$

Liquid Phase

r-component

$$\sigma_r \rho_p \left[W_{pr} \frac{\delta W_{pr}}{\partial r} + \left(\frac{W_{p\theta}}{r} + \omega \right) \frac{\delta W_{pr}}{\partial \theta} - \frac{(W_{p\theta} + r\omega)^2}{r} \right.$$

$$\left. + W_{pz} \frac{\delta W_{pr}}{\partial z} \right] = F_{Bpr} + F_{Vpr} - F_{Ir} \qquad \text{(A.II.46)}$$

θ-component

$$\sigma_r \rho_p \left[W_{pr} \left(\frac{\delta W_{p\theta}}{\partial r} + \omega \right) + \left(\frac{W_{p\theta}}{r} + \omega \right) \frac{\delta W_{p\theta}}{\partial \theta} \right.$$

$$\left. + W_{pr} \left(\frac{W_{p\theta}}{r} + \omega \right) + W_{pz} \frac{\delta W_{p\theta}}{\partial z} \right] = F_{Bp\theta} + F_{Vp\theta} - F_{I\theta} \qquad \text{(A.II.47)}$$

95

z-component

$$\sigma_v \rho_p \left[W_{pr} \frac{\delta W_{pz}}{\partial r} + \left(\frac{W_{p\theta}}{r} + \omega \right) \frac{\delta W_{pz}}{\partial \theta} + W_{pz} \frac{\delta W_{pz}}{\partial z} \right]$$

$$= F_{Bpz} + F_{Vpz} - F_{Iz}$$

(A.II.48)

c) Energy Conservation Equations:

Gas Phase

$$(1 - \sigma_v) \rho_g \left[W_{gr} \frac{\delta h_g}{\partial r} + \left(\frac{W_{g\theta}}{r} + \omega \right) \frac{\delta h_g}{\partial \theta} + W_{gz} \frac{\delta h_g}{\partial z} \right]$$

$$= \Phi_g + \Phi_I + \bar{P}_g + W_{gr} \frac{\delta p_g}{\partial r} + \left(\frac{W_{g\theta}}{r} + \omega \right) \frac{\delta p_g}{\partial \theta}$$

(A.II.49)

$$+ W_{gz} \frac{\delta p_g}{\partial z} - \frac{\delta q'_{gr}}{\partial r} - \frac{\delta q'_{Ir}}{\partial r} - \frac{1}{r} \left[\frac{\delta q'_{g\theta}}{\partial \theta} + \frac{\delta q'_{I\theta}}{\partial \theta} \right]$$

$$- \frac{\delta q'_{gz}}{\partial z} - \frac{\delta q'_{Iz}}{\partial z}$$

96

Liquid Phase

$$\sigma_v \rho_P \left[W_{Pr} \frac{\delta u_P}{\partial r} + \left(\frac{W_{P\theta}}{r} + \omega \right) \frac{\delta u_P}{\partial \theta} + W_{Pz} \frac{\delta u_P}{\partial z} \right] = \mathcal{F}_P - \mathcal{F}_I$$

$$+ \bar{P}_P - \frac{\delta g'_{Pr}}{\partial r} - \frac{1}{r} \left(\frac{\delta g'_{P\theta}}{\partial \theta} - \frac{\delta g'_{I\theta}}{\partial \theta} \right) - \frac{\delta g'_{Pz}}{\partial z} + \frac{\delta g'_{Ir}}{\partial r} + \frac{\delta g'_{Iz}}{\partial z}$$

(A.II.50)

d) Variation of σ_v with respect to the three coordinate directions:

r-direction

The equation is obtained as follows. The θ-component and the z-component gas phase momentum conservation equations are differentiated with respect to θ and z, respectively. Next, the r-component gas phase momentum conservation equation is solved in terms of ($1 - \sigma_v$). These three equations are then combined with the gas phase mass conservation equation to obtain the final result.

$$\frac{\delta \sigma_v}{\partial r} = - \frac{\dot{m}_v}{\rho_g W_{gr}} + \frac{1}{\rho_g W_{gr}} \left(\frac{W_{g\theta}}{r} + \omega \right) \frac{\delta}{\partial \theta} \left[F_{Bg\theta} + F_{Vg\theta} + F_{I\theta} - \frac{1}{r} \frac{\delta p_g}{\partial \theta} \right] \times$$

$$\left[W_{gr} \left(\frac{\delta W_{g\theta}}{\partial r} + \omega \right) + \left(\frac{W_{g\theta}}{r} + \omega \right) \frac{\delta W_{g\theta}}{\partial \theta} + W_{gr} \left(\frac{W_{g\theta}}{r} + \omega \right) + \left(\frac{\delta W_{g\theta}}{\partial z} \right) W_{gz} \right]^{-1}$$

$$+ \frac{W_{gz}}{\rho_g W_{gr}} \frac{\delta}{\partial z} \left[F_{Bgz} + F_{Vgz} + F_{Iz} - \frac{\delta p_g}{\partial z} \right] \left[W_{gr} \frac{\delta W_{gz}}{\partial r} + \left(\frac{W_{g\theta}}{r} + \omega \right) \frac{\delta W_{gz}}{\partial \theta} \right.$$

97

$$+ W_{gz} \frac{\delta W_{gz}}{\partial z} \Bigg]^{-1} + \left[F_{B_{gr}} + F_{r_{gr}} + F_{I_r} - \frac{\delta P_g}{\partial r} \right] \frac{1}{r \rho_g^2 W_{gr}} \left[W_{gr} \frac{\delta W_{g_1}}{\partial r} \right.$$

$$+ \left(\frac{W_{g\theta}}{r} + \omega \right) \frac{\delta W_{gr}}{\partial \theta} - \frac{(W_{g\theta} + r\omega)^2}{r} + W_{gz} \frac{\delta W_{gr}}{\partial z} \Bigg]^{-1} \times$$

$$\left\{ \frac{\delta}{\partial r} (r \rho_g W_{gr}) + \rho_g \frac{\delta W_{g\theta}}{\partial \theta} + \rho_g \frac{\delta (r W_{gz})}{\partial z} - \rho_g (W_{g\theta} + r\omega) \right.$$

$$\frac{\delta}{\partial \theta} \left[W_{gr} \left(\frac{\delta W_{g\theta}}{\partial r} + \omega \right) + \left(\frac{W_{g\theta}}{r} + \omega \right) \frac{\delta W_{g\theta}}{\partial \theta} - W_{gr} \left(\frac{W_{g\theta}}{r} + \omega \right) \right. \qquad \text{(A.II.51)}$$

$$+ W_{gz} \frac{\delta W_{g\theta}}{\partial z} \Bigg] - r \rho_g W_{gz} \frac{\delta}{\partial z} \left[W_{gr} \frac{\delta W_{gz}}{\partial r} + \left(\frac{W_{g\theta}}{r} + \omega \right) \frac{\delta W_{gz}}{\partial \theta} \right.$$

$$+ W_{gz} \frac{\delta W_{gz}}{\partial z} \Bigg] \left[W_{gr} \frac{\delta W_{gz}}{\partial r} + \left(\frac{W_{g\theta}}{r} + \omega \right) \frac{\delta W_{gz}}{\partial \theta} + W_{gz} \frac{\delta W_{gz}}{\partial z} \right]^{-1} \Bigg\}$$

θ-direction

This equation is obtained as follows. The r-component and the z-component gas phase momentum conservation equations are differentiated with respect to r and z, respectively. Next, the θ-component gas phase momentum equation is solved in terms of $(1 - \sigma_v)$. These three equations are then combined with the gas phase mass conservation equation to obtain the final result.

98

$$\frac{\delta \sigma_r}{\delta \theta} = \frac{-r m_r}{\rho_g (W_{g\theta} + r\omega)} + \frac{r}{\rho_g (W_{g\theta} + r\omega)} \frac{\delta}{\delta r} \left[F_{Bg r} + F_{Vg r} + F_{I r} - \frac{\delta P_g}{\delta r} \right] \times$$

$$\left[W_{gr} \frac{\delta W_{gr}}{\delta r} + \left(\frac{W_{g\theta}}{r} + \omega \right) \frac{\delta W_{gr}}{\delta \theta} - \frac{(W_{g\theta} + r\omega)^2}{r} + W_{gz} \frac{\delta W_{gr}}{\delta z} \right]^{-1}$$

$$+ \frac{\delta}{\delta z} \left[F_{Bg z} + F_{Vg z} + F_{I z} - \frac{\delta P_g}{\delta z} \right] \frac{r W_{gz}}{\rho_g (W_{g\theta} + r\omega)} \left[W_{gr} \frac{\delta W_{gz}}{\delta r} + \left(\frac{W_{g\theta}}{r} + \omega \right) \frac{\delta W_{gz}}{\delta \theta} \right.$$

$$\left. + W_{gz} \frac{\delta W_{gz}}{\delta z} \right]^{-1} \cdot \left[F_{Bg\theta} + F_{Vg\theta} + F_{I\theta} - \frac{1}{r} \frac{\delta P_g}{\delta \theta} \right] \frac{1}{\rho_g^2 (W_{g\theta} + r\omega)} \times$$

$$\left[W_{gr} \left(\frac{\delta W_{g\theta}}{\delta r} + \omega \right) + \left(\frac{W_{g\theta}}{r} + \omega \right) \frac{\delta W_{g\theta}}{\delta \theta} + W_{gr} \left(\frac{W_{g\theta}}{r} + \omega \right) \right. \qquad \text{(A.II.52)}$$

$$\left. + W_{gz} \frac{\delta W_{g\theta}}{\delta z} \right]^{-1} \left\{ \rho_g \frac{\delta}{\delta r} (r W_{gr}) + \frac{\delta}{\delta \theta} (\rho_g W_{g\theta}) + \rho_g \frac{\delta}{\delta z} (r W_{gz}) \right.$$

$$- r \rho_g W_{gr} \frac{\delta}{\delta r} \left[W_{gr} \frac{\delta W_{gr}}{\delta r} + \left(\frac{W_{g\theta}}{r} + \omega \right) \frac{\delta W_{gr}}{\delta \theta} - \frac{(W_{g\theta} + r\omega)^2}{r} + W_{gz} \frac{\delta W_{gr}}{\delta z} \right] \times$$

$$\left[W_{gr} \frac{\delta W_{gr}}{\delta r} + \left(\frac{W_{g\theta}}{r} + \omega \right) \frac{\delta W_{gr}}{\delta \theta} - \frac{(W_{g\theta} + r\omega)^2}{r} + W_{gz} \frac{\delta W_{gr}}{\delta z} \right]^{-1}$$

$$\frac{-\delta}{\delta z} \left[W_{gr} \frac{\delta W_{gz}}{\delta r} + \left(\frac{W_{g\theta}}{r} + \omega \right) \frac{\delta W_{gz}}{\delta \theta} + W_{gz} \frac{\delta W_{gz}}{\delta z} \right] r \rho_g W_{gz} \times$$

$$\left. \left[W_{gr} \frac{\delta W_{gz}}{\delta r} + \left(\frac{W_{g\theta}}{r} + \omega \right) \frac{\delta W_{gz}}{\delta \theta} + W_{gz} \frac{\delta W_{gz}}{\delta z} \right]^{-1} \right\}$$

z-direction

This equation is obtained as follows. The r-component and the θ-compone̶nt gas phase momentum conservation equations are differentiated with respect to r and θ, respectively. Next the z-component g̶·s phase momentum conservation equation is solved in terms of ($1 - \sigma_r$). These three equations are then combined with the gas phase mass conservation equation to obtain the final result.

$$
\frac{\delta \sigma_r}{\partial z} = -\frac{m_r}{\rho_g W_{gz}} + \frac{1}{\rho_g W_{gz}}\left(\frac{W_{g\theta}}{r}+\omega\right)\frac{\delta}{\partial\theta}\left[F_{\theta g\theta} + F_{r,\theta} + F_{\theta} - \frac{1}{r}\frac{\delta P_g}{\partial\theta}\right]\times
$$

$$
\left[W_{gr}\left(\frac{\delta W_{g\theta}}{\partial r}+\omega\right) + \left(\frac{W_{g\theta}}{r}+\omega\right)\frac{\delta W_{g\theta}}{\partial\theta} + W_{gr}\left(\frac{W_{g\theta}}{r}+\omega\right) + W_{gz}\frac{\delta W_{g\theta}}{\partial z}\right]^{-1}
$$

$$
+ \frac{W_{gr}}{\rho_g W_{gz}}\frac{\delta}{\partial r}\left[F_{\theta gr} + F_{vgr} + F_{I_r} - \frac{\delta P_g}{\partial r}\right]\left[W_{gr}\frac{\delta W_{gr}}{\partial r} + \left(\frac{W_{g\theta}}{r}+\omega\right)\frac{\delta W_{gr}}{\partial\theta}\right.
$$

$$
\left.- \frac{(W_{g\theta}+r\omega)^2}{r} + W_{gz}\frac{\delta W_{gr}}{\partial z}\right]^{-1} + \left[F_{\theta gz} + F_{vgz} + F_{Iz} - \frac{\delta P_g}{\partial z}\right]\frac{1}{r\sigma_g^2 W_{gz}}
$$

$$
\left[W_{gr}\frac{\delta W_{gz}}{\partial r} + \left(\frac{W_{g\theta}}{r}+\omega\right)\frac{\delta W_{gz}}{\partial\theta} + W_{gz}\frac{\delta W_{gz}}{\partial z}\right]^{-1} \tag{A.II.53}
$$

$$
\left\{\rho_g\frac{\delta(1\cdot W_{gr})}{\partial r} + \rho_g\frac{\delta W_{g\theta}}{\partial\theta} + \frac{\delta}{\partial z}(r\sigma_g W_{gz}) - r\rho_g W_{gr}\frac{\delta}{\partial r}\left[W_{gr}\frac{\delta W_{gr}}{\partial r}\right.\right.
$$

$$
\left.+\left(\frac{W_{g\theta}}{r}+\omega\right)\frac{\delta W_{gr}}{\partial\theta} - \frac{(W_{g\theta}+r\omega)^2}{r} + W_{gz}\frac{\delta W_{gr}}{\partial z}\right]\times\left[W_{gr}\frac{\delta W_{gr}}{\partial r}\right.
$$

$$+ \left(\frac{W_{g\theta}}{r} + \omega \right) \frac{\delta W_{gr}}{\delta \theta} - \frac{(W_{g\theta} + r\omega)^2}{r} + W_{gz} \frac{\delta W_{gr}}{\delta z} \right]^{-1} - \rho_g \left(W_{g\theta} + r\omega \right) \times$$

$$\frac{\delta}{\delta \theta} \left[W_{gr} \left(\frac{\delta W_{g\theta}}{\delta r} + \omega \right) + \left(\frac{W_{g\theta}}{r} + \omega \right) \frac{\delta W_{g\theta}}{\delta \theta} + W_{gr} \left(\frac{W_{g\theta}}{r} + \omega \right) + W_{gz} \frac{\delta W_{g\theta}}{\delta z} \right] \times$$

$$\left[W_{gr} \left(\frac{\delta W_{g\theta}}{\delta r} + \omega \right) + \left(\frac{W_{g\theta}}{r} + \omega \right) \frac{\delta W_{g\theta}}{\delta \theta} + W_{gr} \left(\frac{W_{g\theta}}{r} + \omega \right) + W_{gz} \frac{\delta W_{g\theta}}{\delta z} \right]^{-1} \Bigg\}$$

e) Equilibrium Equations:

Gas Phase

These equations are obtained by combining (A.II.16) with each of the three component gas phase momentum conservation equations.

r-component

$$(1 - \sigma_r) \rho_g \left[W_{gz} \left(\frac{\delta W_{gr}}{\delta z} - \frac{\delta W_{gz}}{\delta r} \right) - (W_{g\theta} + r\omega) \left(\frac{\delta W_{g\theta}}{\delta r} + 2\omega + \frac{W_{g\theta}}{r} - \frac{1}{r} \frac{\delta W_{gr}}{\delta \theta} \right) \right]$$

$$= -(1 - \sigma_r) \rho_g \frac{\delta H_g}{\delta r} + T_g \frac{\delta S_g}{\delta r} + T_{gp} \frac{\delta S_{\mathcal{I}}}{\delta r} \qquad \text{(A.II.54)}$$

$$- \frac{\delta \varsigma_g}{\delta r} - \frac{\delta \varsigma_{\mathcal{I}}}{\delta r} + F_{Bgr} + F_{Vgr} + F_{\mathcal{I}r}$$

101

θ-component

$$(1-\sigma_r)\rho_3\left[W_{32}\left(\frac{\delta W_{30}}{\partial z}-\frac{1}{r}\frac{\delta W_{32}}{\partial \theta}\right)+W_{3r}\left(\frac{\delta W_{30}}{\partial r}+2v_-+\frac{W_{30}}{r}-\frac{1}{r}\frac{\delta W_{3r}}{\partial \theta}\right)\right]$$

$$=\left[-(1-\sigma_r)\rho_3\frac{\delta H_3}{\partial \theta}+T_3\frac{\delta S_{33}}{\partial \theta}+T_{3p}\frac{\delta S_{33}}{\partial \theta}-\frac{\delta_{13}}{\partial \theta}-\frac{\delta_{32}}{\partial \theta}\right]\frac{1}{r}$$

$$\hspace{8cm}\text{(A.II.55)}$$

$$+F_{B_{30}}+F_{V_{30}}+F_{I\theta}$$

z-component

$$(1-\sigma_r)\rho_3\left[W_{3r}\left(\frac{\delta W_{32}}{\partial r}-\frac{\delta W_{3r}}{\partial z}\right)-(W_{30}+r\omega)\left(\frac{\delta W_{30}}{\partial z}-\frac{1}{r}\frac{\delta W_{32}}{\partial \theta}\right)\right]$$

$$=-(1-\sigma_r)\rho_3\frac{\delta H_3}{\partial z}+T_3\frac{\delta_{33}}{\partial z}+T_{3p}\frac{\delta_{31}}{\partial z}-\frac{\delta_{33}}{\partial z}$$

$$\hspace{8cm}\text{(A.II.56)}$$

$$-\frac{\delta_{31}}{\partial z}+F_{B_{32}}+F_{V_{32}}+F_{Iz}$$

Liquid Phase

    These equations are obtained by combining (A.II.22) with each of the three component liquid phase momentum conservation equations.

102

r-component

$$\sigma_v \rho_p \left[W_{p2} \left(\frac{\delta W_{pr}}{\partial z} - \frac{\delta W_{pz}}{\partial r} \right) - \left(W'_{p\theta} + r\omega \right) \left(\frac{\delta W_{p\theta}}{\partial r} + \frac{W_{p\theta}}{r} + 2\omega - \frac{1}{r} \frac{\delta W_{pr}}{\partial \theta} \right) \right]$$

$$= - \sigma_v \rho_p \frac{\delta U_p}{\partial r} + T_p \frac{\delta s_p}{\partial r} - T_{3p} \frac{\delta s_{I}}{\partial r} - \frac{\delta \gamma_p}{\partial r} + \frac{\delta \gamma_{I}}{\partial r} \qquad \text{(A.II.57)}$$

$$+ \Gamma_{B_{pr}} + \Gamma_{V_{pr}} - \Gamma_{I r}$$

θ-component

$$\sigma_v \rho_p \left[W_{p2} \left(\frac{\delta W_{p\theta}}{\partial z} - \frac{1}{r} \frac{\delta W_{pz}}{\partial \theta} \right) + W_{pr} \left(\frac{\delta W_{p\theta}}{\partial r} + \frac{W_{p\theta}}{r} + 2\omega - \frac{1}{r} \frac{\delta W_{pr}}{\partial \theta} \right) \right]$$

$$= \frac{1}{r} \left[-\sigma_v \rho_p \frac{\delta U_p}{\partial \theta} + T_p \frac{\delta s_p}{\partial \theta} - T_{3p} \frac{\delta s_{I}}{\partial \theta} - \frac{\delta \gamma_p}{\partial \theta} + \frac{\delta \gamma_{I}}{\partial \theta} \right] \qquad \text{(A.II.58)}$$

$$+ \Gamma_{B_{p\theta}} + \Gamma_{V_{p\theta}} - \Gamma_{I \theta}$$

103

z-component

$$\sigma_r \rho_\rho \left[W_{\rho r} \left(\frac{\delta W_{\rho z}}{\partial r} - \frac{\delta W_{\rho r}}{\partial z} \right) - \left(W_{\rho \vartheta} + r w \right) \left(\frac{\delta W_{\rho \vartheta}}{\partial z} - \frac{1}{r} \frac{\delta W_{\rho z}}{\partial \vartheta} \right) \right]$$

$$= - \sigma_r \rho_\rho \frac{\delta U_\rho}{\partial z} + T_\rho \frac{\delta s_\rho}{\partial z} - T_{\vartheta\rho} \frac{\delta s_\vartheta}{\partial z} - \frac{\delta y_\vartheta}{\partial z} + \frac{\delta g_\vartheta}{\partial z} \qquad (A.II.59)$$

$$+ F_{B\rho z} + F_{V\rho z} - F_{Iz}$$

II.4. Axisymmetric Flow Equations in Cylindrical Coordinates

a) Mass Conservation Equations:

Gas Phase

$$\frac{1}{r} \frac{\delta}{\partial r} \left(r [1 - \sigma_r] \rho_g W_{gr} \right) + \frac{\delta}{\partial z} \left([1 - \sigma_r] \rho_g W_{gz} \right)$$

$$= \dot{m}_v \qquad (A.II.60)$$

Liquid Phase

$$\frac{1}{r} \frac{\delta}{\partial r} \left(r \sigma_v \rho_\rho W_{\rho r} \right) + \frac{\delta}{\partial z} \left(\sigma_r \rho_\rho W_{\rho z} \right) = - \dot{m}_v$$

$$(A.II.61)$$

b) Momentum Conservation Equations:

Gas Phase

r-component

$$(1 - \sigma_r)\rho_g \left[W_{gr} \frac{\delta W_{gr}}{\delta r} - \frac{(W_{g\theta} + r\omega)^2}{r} + W_{gz} \frac{\delta W_{gr}}{\delta z} \right]$$

(A.II.62)

$$= -\frac{\delta P_g}{\delta r} + F_{B_{gr}} + F_{V_{gr}} + F_{Ir}$$

θ-component

$$(1 - \sigma_r)\rho_g \left[W_{gr} \left(\frac{\delta W_{g\theta}}{\delta r} + \omega \right) + W_{gr} \left(\frac{W_{g\theta}}{r} + \omega \right) \right.$$

(A.II.63)

$$\left. + W_{gz} \frac{\delta W_{g\theta}}{\delta z} \right] = F_{B_{g\theta}} + F_{V_{g\theta}} + F_{I\theta}$$

z-component

$$(1 - \sigma_r)\rho_g \left[W_{gr} \frac{\delta W_{gz}}{\delta r} + W_{gz} \frac{\delta W_{gz}}{\delta z} \right] = -\frac{\delta P_g}{\delta z}$$

(A.II.64)

$$+ F_{B_{gz}} + F_{V_{gz}} + F_{Iz}$$

Liquid Phase

r-component

$$\sigma_r \rho_\ell \left[W_{\ell r} \frac{\delta W_{\ell r}}{\delta r} - \frac{(W_{\ell\theta} + r\omega)^2}{r} + W_{\ell z} \frac{\delta W_{\ell r}}{\delta z} \right]$$

$$= F_{B_{pr}} + F_{\gamma_{pr}} - F_{Ir} \tag{A.II.65}$$

θ-component

$$\sigma_r \rho_p \left[W_{pr} \left(\frac{\delta W_{p\theta}}{\delta r} + \omega \right) + W_{pr} \left(\frac{W_{p\theta} + \omega}{r} \right) \right.$$

$$\left. + W_{pz} \frac{\delta W_{p\theta}}{\delta z} \right] = F_{B_{p\theta}} + F_{\gamma_{p\theta}} - F_{I\theta} \tag{A.II.66}$$

z-component

$$\sigma_v \rho_p \left[W_{pr} \frac{\delta W_{pz}}{\delta r} + W_{pz} \frac{\delta W_{pz}}{\delta z} \right]$$

$$= F_{B_{pz}} + F_{\gamma_{pz}} - F_{Iz} \tag{A.II.67}$$

c) Energy Conservation Equations:

Gas Phase

$$(1 - \sigma_r) \rho_g \left[W_{gr} \frac{\delta h_g}{\delta r} + W_{gz} \frac{\delta h_g}{\delta z} \right] = \Phi_g + \Phi_I + \bar{P}_g + W_{gr} \frac{\delta P_g}{\delta r}$$

$$+ W_{gz} \frac{\delta P_g}{\delta z} - \frac{\delta q'_{gr}}{\delta r} - \frac{\delta q'_{Ir}}{\delta r} - \frac{\delta q'_{gz}}{\delta z} - \frac{\delta q'_{Iz}}{\delta z} \tag{A.II.68}$$

106

<u>Liquid Phase</u>

$$\sigma_v \, \rho_p \left[W_{pr} \, \frac{\delta u_{\ell p}}{\partial r} + W'_{pz} \, \frac{\delta u_{\ell 2}}{\partial z} \right] = \Phi_p - \Phi_I + \bar{P}_{I'}$$

$$- \frac{\delta q'_{pr}}{\partial r} + \frac{\delta q'_{Ir}}{\partial r} - \frac{\delta q'_{pz}}{\partial z} + \frac{\delta q'_{Iz}}{\partial z}$$

(A.II.69)

d) Variation of σ_v with respect to the three coordinate directions:

<u>r-direction</u>

$$\frac{\delta \sigma_r}{\partial r} = - \frac{\dot{m}_v}{\rho_g W_{gr}} + \frac{W_{gz}}{\rho_g W_{gr}} \frac{\delta}{\partial z} \left[F_{Bgz} + F_{Vgz} + F_{Iz} - \frac{\delta P_g}{\partial z} \right] \times$$

$$\left[W_{gr} \frac{\delta W_{gz}}{\partial r} + W_{gz} \frac{\delta W_{gz}}{\partial z} \right]^{-1} + \frac{1}{r \rho_g^2 W_{gr}} \left[F_{Bgr} + F_{Vgr} + F_{Ir} - \frac{\delta P_g}{\partial r} \right] \times$$

$$\left[W_{gr} \frac{\delta W_{gr}}{\partial r} + W_{gz} \frac{\delta W_{gr}}{\partial z} - \frac{(W_{g\theta} + r\omega)^2}{r} \right]^{-1} .$$

(A.II.70)

$$\left\{ \frac{\delta}{\partial r} (r \rho_g W_{gr}) + \rho_g \frac{\delta (r W_{gz})}{\partial z} - r \rho_g W_{gz} \frac{\delta}{\partial z} \left[W_{gr} \frac{\delta W_{gz}}{\partial r} + W_{gz} \frac{\delta W_{gz}}{\partial z} \right] : \right.$$

$$\left. \left[W_{gr} \frac{\delta W_{gz}}{\partial r} + W_{gz} \frac{\delta W_{gz}}{\partial z} \right]^{-1} \right\}$$

107

<u>θ-direction</u>

$$\frac{\delta \sigma_v}{\partial \theta} = 0 \tag{A.II.71}$$

<u>z-direction</u>

$$\frac{\delta \sigma_v}{\partial z} = -\frac{m_v}{\rho_g W_{gz}} + \frac{W_{gr}}{\rho_g W_{gz}} \frac{\delta}{\partial r} \left[F_{Bgr} + F_{vgr} + F_{Ir} - \frac{\delta P_g}{\partial r} \right] \times$$

$$\left[W_{gr} \frac{\delta W_{gr}}{\partial r} - \frac{(W_{g\theta} + r\omega)^2}{r} + W_{gz} \frac{\delta W_{gr}}{\partial z} \right]^{-1} + \frac{1}{r \rho_g^2 W_{gz}} \,$$

$$\left[F_{Bgz} + F_{vgz} + F_{Iz} - \frac{\delta P_g}{\partial z} \right] \left[W_{gr} \frac{\delta W_{gz}}{\partial r} + W_{gz} \frac{\delta W_{gz}}{\partial z} \right]^{-1} \times$$

$$\left\{ \rho_g \frac{\delta}{\partial r}(r W_{gr}) + \frac{\delta}{\partial z} (r \rho_g W_{gz}) - r \rho_g W_{gr} \, \times \right. \tag{A.II.72}$$

$$\frac{\delta}{\partial r} \left[W_{gr} \frac{\delta W_{gr}}{\partial r} - \frac{(W_{g\theta} + r\omega)^2}{r} + W_{gz} \frac{\delta W_{gr}}{\partial z} \right] \,$$

108

$$\left[W_{gr} \frac{\delta W_{gr}}{\delta r} - \frac{(W_{g\theta} + rw)^2}{r} + W_{gz} \frac{\delta W_{gr}}{\delta z} \right]^{-1} \Bigg\}$$

e) Equilibrium Equations:

Gas Phase

r-component

$$(1-\sigma_r)\rho_g \left[W_{gz} \left(\frac{\delta W_{gr}}{\delta z} - \frac{\delta W_{gz}}{\delta r} \right) - (W_{g\theta} + rw) \times \right.$$

$$\left. \left(\frac{\delta W_{g\theta}}{\delta r} + 2w + \frac{W_{g\theta}}{r} \right) \right] = -(1-\sigma_r)\rho_g \frac{\delta H_g}{\delta r} \qquad \text{(A.II.73)}$$

$$+ T_g \frac{\delta s_g}{\delta r} + T_{gp} \frac{\delta s_I}{\delta r} - \frac{\delta q_g}{\delta r} - \frac{\delta q_I}{\delta r} + F_{Bgr} + F_{Vgr} + F_{Ir}$$

θ-component

$$(1-\sigma_r)\rho_g \left[W_{gz} \frac{\delta W_{g\theta}}{\delta z} + W_{gr} \left(\frac{\delta W_{g\theta}}{\delta r} + 2w + \frac{W_{g\theta}}{r} \right) \right]$$

$$= F_{Bg\theta} + F_{Vg\theta} + F_{I\theta} \qquad \text{(A.II.74)}$$

z-component

$$(1 - \sigma_r) \rho_g \left[W_{gr} \left(\frac{\delta W_{gz}}{\partial r} - \frac{\delta W_{gr}}{\partial z} \right) - (W_{g\theta} + r\omega) \left(\frac{\delta W_{g\theta}}{\partial z} \right) \right]$$

$$= -(1 - \sigma_r) \rho_g \frac{\delta H_g}{\partial z} + T_g \frac{\delta s_g}{\partial z} + T_{gp} \frac{\delta s_I}{\partial z} \qquad (A.II.75)$$

$$- \frac{\delta q_g}{\partial z} - \frac{\delta q_I}{\partial z} + F_{Bgz} + F_{\gamma gz} + F_{Iz}$$

Liquid Phase

r-component

$$\sigma_r \rho_p \left[W_{pz} \left(\frac{\delta W_{pr}}{\partial z} - \frac{\delta W_{pz}}{\partial r} \right) - (W_{p\theta} + r\omega) \times \right.$$

$$\left. \left(\frac{\delta W_{p\theta}}{\partial r} + 2\omega + \frac{W_{p\theta}}{r} \right) \right] = -\sigma_r \rho_p \frac{\delta U_p}{\partial r} \qquad (A.II.76)$$

$$+ T_p \frac{\delta s_p}{\partial r} - T_{gp} \frac{\delta s_I}{\partial r} - \frac{\delta q_p}{\partial r} + \frac{\delta q_I}{\partial r} + F_{Bpr} + F_{\gamma pr} - F_{Ir}$$

110

θ-component

$$\sigma_v \rho_p \left[W_{pz} \frac{\delta W_{p\theta}}{\partial z} + W_{pr} \left(\frac{\delta W_{p\theta}}{\partial r} + 2\omega + \frac{W_{p\theta}}{r} \right) \right]$$

(A.II.77)

$$= F_{Bp\theta} + F_{vp\theta} - F_{I\theta}$$

z-component

$$\sigma_v \rho_p \left[W_{pr} \left(\frac{\delta W_{pz}}{\partial r} - \frac{\delta W_{pr}}{\partial z} \right) - (W_{p\theta} + r\omega) \frac{\delta W_{p\theta}}{\partial z} \right]$$

(A.II.78)

$$= -\sigma_r \rho_p \frac{\delta U_p}{\partial z} + T_p \frac{\delta s_p}{\partial z} - T_{gp} \frac{\delta s_I}{\partial z} - \frac{\delta q_p}{\partial z}$$

$$- \frac{\delta q_I}{\partial z} + F_{Bpz} + F_{vpz} - F_{Iz}$$